



Delft University of Technology

## Natronoglorus mannanivorans gen. nov., sp. nov., beta-1,4-mannan utilizing natronoarchaea from hypersaline soda lakes

Sorokin, Dmitry Y.; Elcheninov, Alexander G.; Bale, Nicol J.; Sinnighe Damsté, Jaap S.; Kublanov, Ilya V.

**DOI**

[10.3389/fmcb.2024.1364606](https://doi.org/10.3389/fmcb.2024.1364606)

**Publication date**

2024

**Document Version**

Final published version

**Published in**

Frontiers in Microbiology

**Citation (APA)**

Sorokin, D. Y., Elcheninov, A. G., Bale, N. J., Sinnighe Damsté, J. S., & Kublanov, I. V. (2024). Natronoglorus mannanivorans gen. nov., sp. nov., beta-1,4-mannan utilizing natronoarchaea from hypersaline soda lakes. *Frontiers in Microbiology*, 15, Article 1364606.  
<https://doi.org/10.3389/fmcb.2024.1364606>

**Important note**

To cite this publication, please use the final published version (if applicable).

Please check the document version above.

**Copyright**

Other than for strictly personal use, it is not permitted to download, forward or distribute the text or part of it, without the consent of the author(s) and/or copyright holder(s), unless the work is under an open content license such as Creative Commons.

**Takedown policy**

Please contact us and provide details if you believe this document breaches copyrights.  
We will remove access to the work immediately and investigate your claim.



## OPEN ACCESS

## EDITED BY

Mohammad Ali Amoozegar,  
University of Tehran, Iran

## REVIEWED BY

Heng-Lin Cui,  
Jiangsu University, China  
Doug Bartlett,  
University of California, San Diego,  
United States

## \*CORRESPONDENCE

Dmitry Y. Sorokin  
✉ soroc@inmi.ru;  
✉ d.sorokin@tudelft.nl

RECEIVED 02 January 2024

ACCEPTED 14 February 2024

PUBLISHED 12 March 2024

## CITATION

Sorokin DY, Elcheninov AG, Bale NJ,  
Sinninghe Damsté JS and Kublanov IV (2024)  
*Natronogloous mannanivorans* gen. nov., sp.  
nov., beta-1,4-mannan utilizing  
natronoarchaea from hypersaline soda lakes.  
*Front. Microbiol.* 15:1364606.  
doi: 10.3389/fmicb.2024.1364606

## COPYRIGHT

© 2024 Sorokin, Elcheninov, Bale, Sinninghe Damsté and Kublanov. This is an open-access article distributed under the terms of the Creative Commons Attribution License (CC BY). The use, distribution or reproduction in other forums is permitted, provided the original author(s) and the copyright owner(s) are credited and that the original publication in this journal is cited, in accordance with accepted academic practice. No use, distribution or reproduction is permitted which does not comply with these terms.

# *Natronogloous mannanivorans* gen. nov., sp. nov., beta-1,4-mannan utilizing natronoarchaea from hypersaline soda lakes

Dmitry Y. Sorokin<sup>1,2\*</sup>, Alexander G. Elcheninov<sup>1</sup>, Nicole J. Bale<sup>3</sup>,  
Jaap S. Sinninghe Damsté<sup>3</sup> and Ilya V. Kublanov<sup>1</sup>

<sup>1</sup>Winogradsky Institute of Microbiology, Research Centre of Biotechnology, Russian Academy of Sciences, Moscow, Russia, <sup>2</sup>Department of Biotechnology, Delft University of Technology, Delft, Netherlands, <sup>3</sup>NIOZ Royal Netherlands Institute for Sea Research, Texel, Netherlands

Beta-mannans are insoluble plant polysaccharides with beta-1,4-linked mannose as the backbone. We used three forms of this polysaccharide, namely, pure mannan, glucomannan, and galactomannan, to enrich haloarchaea, which have the ability to utilize mannans for growth. Four mannan-utilizing strains obtained in pure cultures were closely related to each other on the level of the same species. Furthermore, another strain selected from the same habitats with a soluble beta-1,4-glucan (xyloglucan) was also able to grow with mannan. The phylogenomic analysis placed the isolates into a separate lineage of the new genus level within the family *Natriabaceae* of the class *Halobacteria*. The strains are moderate alkaliphiles, extremely halophilic, and aerobic saccharolytics. In addition to the three beta-mannan forms, they can also grow with cellulose, xylan, and xyloglucan. Functional genome analysis of two representative strains demonstrated the presence of several genes coding for extracellular endo-beta-1,4-mannanase from the GH5\_7 and 5\_8 subfamilies and the GH26 family of glycosyl hydrolases. Furthermore, a large spectrum of genes encoding other glycoside hydrolases that were potentially involved in the hydrolysis of cellulose and xylan were also identified in the genomes. A comparative genomics analysis also showed the presence of similar endo-beta-1,4-mannanase homologs in the cellulotrophic genera *Natronobififorma* and *Halococcoides*. Based on the unique physiological properties and the results of phylogenomic analysis, the novel mannan-utilizing haloarchaea are proposed to be classified into a new genus and species *Natronogloous mannanivorans* gen. nov., sp. nov. with the type strain AArc-m2/3/4 (=JCM 34861=UQM 41565).

## KEYWORDS

hypersaline lakes, haloarchaea, glucomannan, galactomannan, beta-1,4-mannan

## Introduction

Recent extensive studies on the functional diversity of extremely halophilic archaea belonging to the class *Halobacteria* resulted in a significant shift in a longstanding perception of this unique group of extremophiles as copiotrophic dissipotrophs utilizing either rich amino acid mixtures or simple soluble monomeric compounds, such as sugars or organic acids. In particular, it is becoming evidently clear that many haloarchaeal species possess extensive hydrolytic potential against various groups of recalcitrant insoluble

polysaccharides, such as chitin, cellulose, and a range of other neutral glucans (Sorokin et al., 2015, 2018, 2019a,b, 2022a, 2023). In our previous study, we used selective enrichments with a range of soluble and insoluble glucans to obtain pure cultures of haloarchaea utilizing various glucans with different monomers and back-bond structures as growth substrates (Sorokin et al., 2022a). One of the selected groups included five isolates of alkaliphilic haloarchaea that have the ability to grow with beta-mannans, including pure beta-1,4-mannan and its two modifications, glucomannan (with glucose and mannose in the backbone) and galactomannan (with galactose in the side chains). To date, the beta-mannans with backbone have been proven to serve as a growth substrate for three characterized species of haloarchaea: *Natronoarchaeum mannanilyticum* (Shimane et al., 2010) and *Haloarcula mannanilytica* (Enomoto et al., 2020) use galactomannan as a substrate and cellulotrophic *Natronobifirma cellulositropha* uses pure beta-1,4-mannan as a substrate (Sorokin et al., 2018). The latter and the heteropolymeric glucomannan have never been tested before to enrich mannan-utilizing haloarchaea. According to the CAZy database (<http://www.cazy.org>), the only enzymatically characterized mannan-specific glycoside hydrolases (several subfamilies of the GH family 5 and the GH family 26) are known in bacteria and eukarya, mostly in fungi. This finding certainly indicates a substantial gap in the knowledge on the potential presence of functionally active archaeal beta-mannanases and on the identity of archaea that are able to utilize such polymers as growth substrates.

In this study, we provide taxonomic evaluation and functional genome analysis focusing on glycosyl hydrolase families for several strains of haloarchaea, which were previously enriched from neutral and alkaline hypersaline lakes in southwestern Siberia on insoluble beta-1,4-mannans. All mannan-utilizing isolates are closely related, forming a separate lineage within the family *Natrialbaceae*, and are proposed to be classified as *Natronoglorus mannanivorans* gen. nov., sp. nov.

## Materials and methods

### Media and cultivation conditions

Mix surface sediments and brines collected from several hypersaline salt and soda lakes in the Kulunda Steppe (Altai, Russia) were used as inoculum for enrichment cultures. The brine pH (measured with the field pH meter, WWR) in neutral lakes of the chloride-sulfate type ranged from 7.5 to 8.2, and in soda lakes, the pH values ranged from 9.8 to 11. The total salt concentration (measured in the field with a refractometer and verified by the gravimetry in the laboratory) was found to be ranging from 200 to 400 g l<sup>-1</sup>. Before cultivation, the sediment suspension (one part of sediment:nine parts of brines, v:v) was preincubated for 3 days at 28°C on a rotary shaker with the addition of 200 mg l<sup>-1</sup> each of ampicillin and streptomycin to suppress the growth of bacteria. The suspended solids were precipitated by centrifugation and resuspended into two types of base mineral medium containing either 4 M total NaCl at pH 7 or a 3:1 (v:v) mix of 4 M NaCl and sodium-carbonate base with 4 M total Na<sup>+</sup> (the final pH was 9.5). The cultures were supplemented with 1 g l<sup>-1</sup> each of three

types of beta-1,4-mannan (Megazyme, Ireland): pure mannan; glucomannan (beta-1,4 heteropolymer of mannose and glucose with a Gl:Man ratio of 4:1); and galactomannan (beta-1,4-mannan with a side chain decoration of alpha-1,6-linked galactose). The polymers were prepared as 10% suspensions in sterile distilled water and sterilized at 110°C for 30 min, and the enrichments were incubated on a rotary shaker in closed bottles at 37°C until visible substrate degradation (accessed by light microscopy) and the appearance of pink turbidity in the liquid phase occurs. Pure culture isolation was achieved after the plating of final positive serial dilution from single colonies forming the clearance zones on the mannan plates (the mannan suspension was sonicated to reduce the particle size) and showing stable growth in the liquid medium with the beta-1,4-mannan as the sole carbon and energy source.

### Phenotypic characterization

Phase contrast microscopy was performed using Zeiss Axioplane Imaging 2 (Germany). The growth in liquid cultures was monitored OD<sub>600</sub> after 30 min of gravity sedimentation of insoluble particles or directly in the case of soluble substrates. Thin-section electron microscopy was performed for the cells of type strain AArc-m2/3/4 grown either with beta-mannan or xylan, using a JEOL100 instrument (Japan) as described previously (Sorokin et al., 2018). The ability for anaerobic growth was tested in serum bottles sealed with butyl rubber stoppers after the removal of dissolved oxygen and subjected first to “cold boiling” under a vacuum followed by flashing three times with sterile argon gas. Aerobic substrate utilization, pH-salt profiling, and other standard phenotypic testing were performed as described by Sorokin et al. (2022a). Membrane polar lipids and respiratory menaquinones were extracted from freeze-dried biomass of strains AArc-m2/3/4 and AArc-xg1-1 that were grown with cellobiose at 37°C, 4 M total Na<sup>+</sup>, and pH 9.5 until the late exponential growth phase and were resolved by Ultra High Pressure Liquid Chromatography-High Resolution Mass Spectrometry (UHPLCHRMS) using an Agilent 1290 Infinity I UHPLC (ThermoFisher Scientific), as described previously (Bale et al., 2021; Sorokin et al., 2022b).

Growth tests were performed in a basal alkaline medium containing 4 M total Na<sup>+</sup> (1 M as sodium carbonates and 3 M as NaCl) at pH 9.5. Substrates were added at a final concentration of 1 g l<sup>-1</sup> after sterilization from 10% concentrated stocks. In total, 10 ml cultures in 30 ml bottles with screw-capped rubber septum (to prevent evaporation) were incubated on a rotary shaker at 37°C. The growth was monitored by measuring OD<sub>600</sub> against a control without substrate, directly in the case of soluble substrate, and after vigorous homogenization and 10 min stasis to allow particles to sediment in the case of insoluble polysaccharides.

### Genome sequencing and phylogenomic and functional genomic analyses

The genomes of AArc-m2/3/4 and AArc-xg1-1 were sequenced using the MiSeq Illumina platform and assembled as described previously (Sorokin et al., 2022a). Their draft assemblies were

deposited in the GenBank under the numbers GCA\_025517485 and GCA\_025517495, respectively.

For phylogenomic analysis, 122 conserved single copy archaeal protein markers (Rinke et al., 2021) from the *in silico* translated genomes of two mannan-utilizing natronoarchaea, the closest related strains KZCA124 and TS33, and all described species of the family *Natrialbaceae*, were identified and aligned using the GTDB-tk v.1.7.0 with reference data v.202 (Chaumeil et al., 2019). The resulting alignment was treated using trimAL v1.4.1 with -gt 1 option for complete gap elimination (Capella-Gutiérrez et al., 2009). The phylogenomic tree was constructed and drawn using the RAxML v.8.2.12 (the PROTGAMMAILG model, 1,000 rapid bootstrap replications) and iTOL v.6.5.2, respectively (Stamatakis, 2014; Letunic and Bork, 2019). The whole genome comparisons (ANI, AAI, and POPC) were calculated as described earlier (Sorokin et al., 2023).

Functional genome analysis of the glycoside hydrolases (GH) with particular focus on the mannan-hydrolyzing families including the GH5\_7, GH5\_8, and GH26 families in AArc-m2/3/4 and AArc-xg1-1 (as well as the genomes of related strains KZCA124 and TS33) was performed using the dbCAN v.4 (Zhang et al., 2018) with HMMER (Mistry et al., 2013) and Diamond tools (Buchfink et al., 2015) to detect the target GH domains. Additional domains were searched using the InterPro database (Paysan-Lafosse et al., 2023). Gene clusters of AArc-m2/3/4, AArc-xg1-1, and several other species containing genes encoding endo-beta-mannanases were visualized using the gggenes package in R (<https://cran.r-project.org/web/packages/gggenes>). The GH5 and GH26 enzymes of strains AArc-m2/3/4 and AArc-xg1-1 and related proteins found by the NCBI BLAST (the organism list was limited to *Archaea*; the e-value threshold were 1e-10 and 1e-5 for GH5 and GH26, respectively) were used for the phylogenetic reconstruction of the haloarchaeal beta-mannanases. Furthermore, all proteins were analyzed using dbCAN v.4 with HMMER tool to detect target domains; only proteins with target catalytic domains (minimal coverage is 0.4) and some additional carbohydrate-binding domains (minimal coverage is 0.5) were kept in the final protein set. Both sets of sequences (the GH5 and GH26 families) were aligned using MAFFT v.7 with the E-INS-i method (Katoh et al., 2017). The alignments obtained were trimmed using trimAL v1.4.1 with -gt 0.75 (Capella-Gutiérrez et al., 2009). The phylogenetic trees for GH5 and GH26 glycosidases were constructed and decorated as described above for the “ar122”-based phylogenomic tree with a decreased number of bootstrap replications (500).

## Results and discussion

### Enrichment and isolation of pure cultures of mannan-utilizing haloarchaea

Five enrichment cultures (one from neutral salt lakes and four from soda lakes) showed stable growth with four different polymers. The neutral and soda lake enrichments with beta-1,4-mannan yielded strains HArc-m1 and AArc-m2/3/4<sup>T</sup>; the soda lake enrichments with galactomannan yielded strain AArc-glctm5 and with glucomannan yielded strain AArc-gm3/4/5-2. An additional

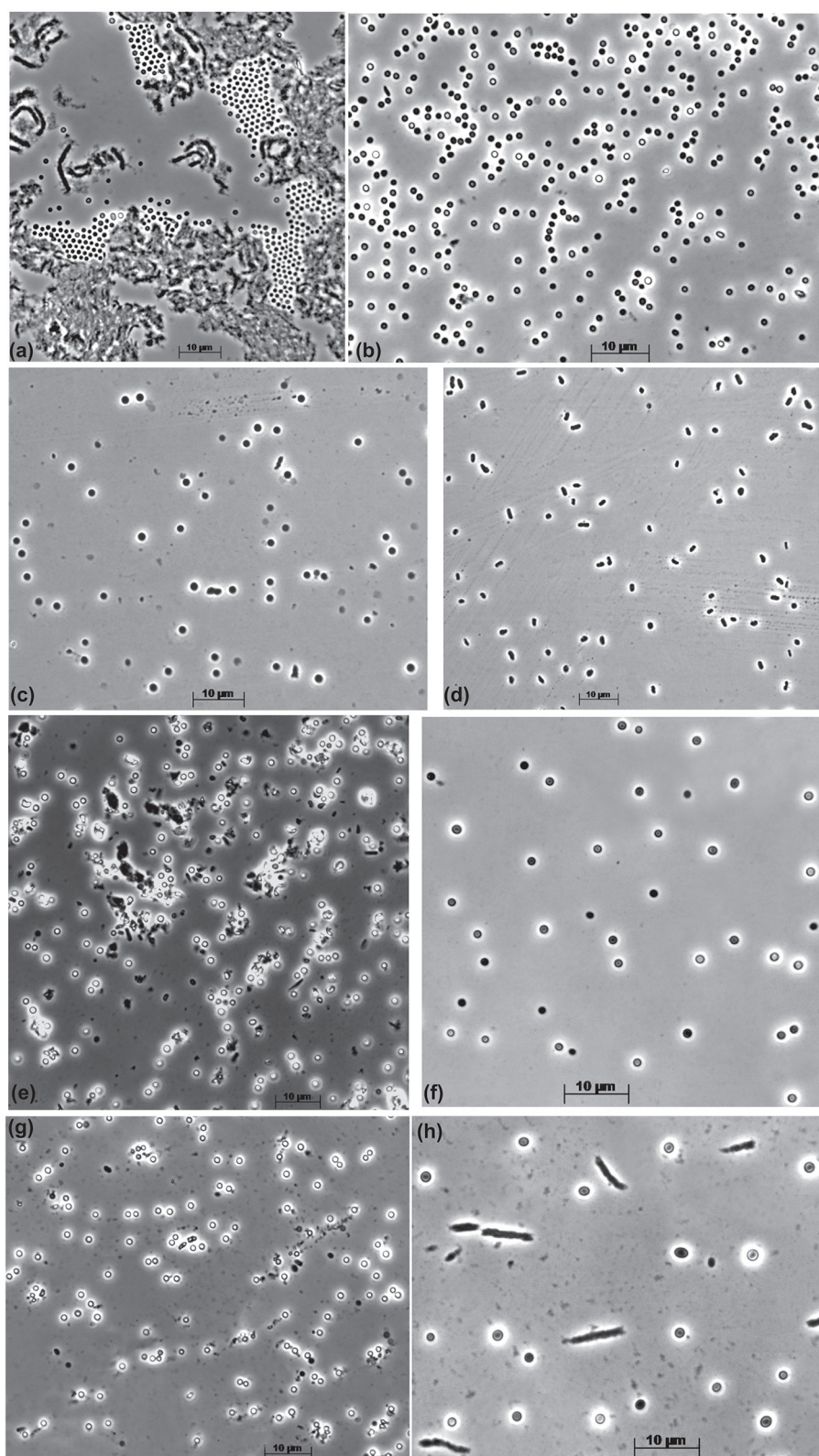
enrichment with xyloglucan provided an additional beta-1,4-mannan-utilizing isolate AArc-xg1-1. It was confirmed that the first four isolates selected with different mannan variations could grow with beta-1,4-mannan. The xyloglucan-yielded isolate AArc-xg1-1 was first identified as a potential mannan utilizer based on its phylogenomic proximity to the mannan-enriched strains and functional genome analysis, and it was later confirmed by a growth test. An interesting fact to note is that the neutral salt lake isolate, HArc-m1, turned out to be identical to its counterpart mannan-selected soda lake natronarchaeon, AArc-m2/3/4, and was confirmed to be able to grow optimally at moderately alkaline conditions used for the enrichment of the soda lake isolates, which is a rare example (at least in our experience). Evidently, two factors might have played a role in such a coincidence: the first is the close proximity of the chloride-sulfate and soda lakes in the southern Kulunda steppe (a few kilometers range) and the second is the unique substrate specialization overruling the significance of the alkali-related adaptation.

### Phenotypic properties

The cells of all mannan-utilizing strains were mostly true non-motile cocci that were ~1 µm in diameter, becoming especially refractive when grown with mannan and cellulose (Figure 1). Thin sectioning electron microscopy revealed a major difference in the cell ultrastructure between the mannan- and xylan-grown cells: the former had a much thicker cell wall consisting of several layers and an extended pseudoperiplasmic space (Figure 2), which resembled the cellulose-growing cells of *Natronobififorma* (Sorokin et al., 2018). It might be due to the necessity of these haloarchaea to interact physically with the insoluble glucans.

Membrane phospholipid profiling of strains AArc-m2/3/4 and AArc-xg1-1 indicated domination of C<sub>20</sub>-C<sub>20</sub> archaeol and C<sub>20</sub>-C<sub>25</sub> extended archaeol as the core, with phosphatidylglycerolphosphate methyl ester (PGP-Me) and phosphatidylglycerol (PG) as the polar heads in equal proportion (Supplementary Table S1). The glyco- and sulfo-lipids were not detected. The majority of respiratory lipoquinones were represented by the saturated MK-8:8 (75 and 95% in AArc-m2/3/4 and AArc-xg1-1, respectively), and the rest was monounsaturated MK-8:7.

The range of polysaccharides supporting the growth of all isolates included beta-1,4 mannan, glucomannan, amorphous cellulose, xyloglucan, xylan, and arabinoxylan, while galactomannan supported only a weak growth with incomplete degradation. Alpha-glucans from the starch family, beta-glucans with the 1,3- and 1,6-backbone, and the beta-fructans did not support the growth of isolates. Active hydrolysis of the beta-mannan and amorphous cellulose can be observed as the formation of clearance zones around the colonies (Supplementary Figure S1). The range of utilized sugars investigated in the strain AArc-m2/3/4<sup>T</sup> included galactose, lactose, trehalose, raffinose, rhamnose, sucrose, cellobiose, maltose, melezitose, and melibiose. Interestingly, mannose and glucose, the monomers of two groups of growth-supporting beta-1,4-glucans, were not among the utilized sugars. Most likely, only oligomers were transported inside the cells.

**FIGURE 1**

Cell morphology of the beta-1,4-mannan-utilizing haloarchaea growing at 4 M Na<sup>+</sup>, pH 9.5, and 37°C. (a, b) Strain AArc-m2/3/4 on mannan [(a) aggregated cells in the solid phase with polymer, (b) free cells]; (c, d) strain AArc-xg1-1 [(c) on mannan, (d) on xyloglucan]; (e) strain HArc-m1 on mannan; (f) strain AArc-glctm5 on mannan; (g, h) strain AArc-gm3/4/5-2 [(g) on mannan, (h) on glucomannan].

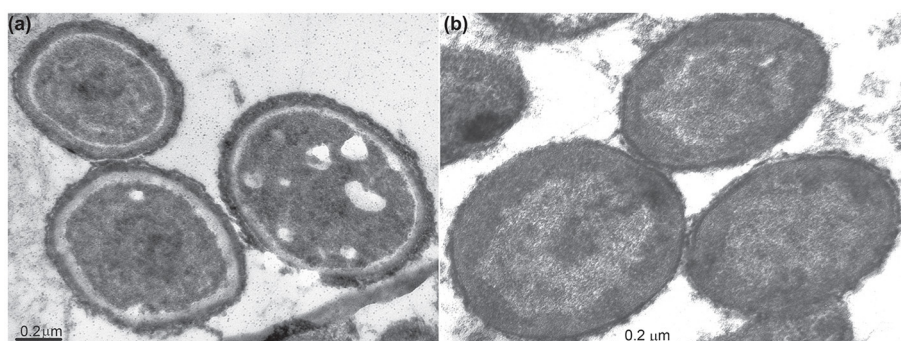


FIGURE 2

Thin-section electron microscopy microphotographs showing an ultrastructural difference of the AArc-m2/3/4 cells grown with beta-1,4-mannan (a) and xylan (b). The mannan-grown cells have an extra external cell layer and extended pseudoperyplasm in comparison to the cells grown on xylan.

Anaerobic growth with cellobiose as a substrate was not observed both at fermentative conditions and in the presence of various electron acceptors, including nitrate, nitrite,  $\text{N}_2\text{O}$ , sulfur, thiosulfate, DMSO, and fumarate. Ammonium and urea, but not nitrate, served as the nitrogen source. The cellobiose-dependent growth at pH 9.5 was not inhibited by streptomycin, ampicillin, kanamycin, vancomycin, and tetracycline at concentrations of up to  $100 \text{ mg l}^{-1}$ .

AArc-m2/3/4<sup>T</sup> grew optimally (with cellobiose at pH 9) at 3.5 M total  $\text{Na}^+$  and with the range from 2.0 to 4.5 M. The pH profiling (with cellobiose at 4 M total  $\text{Na}^+$ ) was performed for the soda lake isolate, AArc-m2/3/4<sup>T</sup>, and for the salt lake isolate, HArc-m1. The former showed a weak growth starting from pH 7.2 and grew up to pH 9.7, while the latter had a lower growth pH limit starting from a minimum of pH 6.8 and was able to grow up to pH 9.5. Both strains grew optimally around pH 9. Thus, they can be qualified as facultatively alkaliphilic extreme halophiles.

## Phylogenetic analysis

The genomes of AArc-m2/3/4 and AArc-xg1-1 contain a single *rrn* operon with the 16S rRNA gene most closely related to the species of the genera *Halovivax* and *Saliphagus* (~95% sequence identity). However, according to the results of the phylogenomic analysis based on 122 archaeal conserved single-copy protein markers, mannan-utilizing isolates formed a distinct clade within the *Natrialbaceae* family neighboring the cellulotrophic genus *Natronobiflora* (Figure 3, Supplementary Figure S2). Furthermore, the whole-genome-based comparative analyses indicated that the novel isolates form an independent lineage of a new genus level within the *Natrialbaceae* (Supplementary Table S2). Average nucleotide identities (ANI) between the AArc-m2/3/4<sup>T</sup> and AArc-xg1-1 strains was 98.5%, which means that they belong to the same species; ANI values between novel isolates and the representatives of the closest genera, *Natronobiflora* and *Saliphagus*, were 77.9 and 77.1%, respectively, and the range for other type species of the *Natrialbaceae* varied from 74.1 to 78.6%. Average amino acid identity (AAI) values between the AArc-m2/3/4<sup>T</sup> and AArc-xg1-1 strains and the type

species of the *Natrialbaceae* ranged from 58.9 to 70.3%, with the highest value being *N. cellulositropha*. These values are significantly below the threshold for the demarcation of genera within the *Natrialbaceae* (76%; de la Haba et al., 2021). The percentage of conserved proteins (POCP) between novel strains and the type species of the *Natrialbaceae* varied from 49.4 to 66.2% with the highest values being *N. cellulositropha* and *Saliphagus infecundisoli*. The highest POCP values were slightly higher than the proposed genus-level threshold of 50% (Qin et al., 2014). However, many authors often indicated that a strict boundary of 50% is not suitable for the demarcation of genera within some taxa (Aliyu et al., 2016; Orata et al., 2018; Wirth and Whitman, 2018). Thus, it is likely that, in the case of the *Natrialbaceae*, the POCP threshold needs to be revised.

## Functional genome analysis

### Beta-mannan utilization potential

The main functional property of the new isolates is the potential to utilize insoluble beta-1,4-mannans and beta-1,4-glucans (cellulose) as a growth substrate. The two sequenced genomes contained a very similar array of genes encoding the key glycoside hydrolases that were potentially involved in the unique substrate specificity of the novel natronoarchaea. A most interesting group of such enzymes included beta-1,4-mannanases belonging to the families GH26 (one enzyme), GH5\_7 (four enzymes, two of them with a carbohydrate binding domain, CBM), and GH5\_8 (one enzyme with a CBM) (Table 1). All six proteins have TAT translocation signals (i.e., are extracellular) and are co-located in two large genomic islands together with the genes coding for multiple endo-beta-1,4-glucanases from the GH5 superfamily, which is most likely responsible for cellulose degradation and/or endo-beta-1,4-xylanases from the GH10 family.

The first cluster contains genes of three endo-beta-1,4-mannosidases from the GH5\_7 and GH5\_8 subfamilies and the GH26 family and a beta-mannosidase from the GH2 family (Figure 4A). Moreover, endo-alpha-1,5-L-arabinanase from the GH43 family, a putative enzyme from the GH109 family (homologous to various sugar dehydrogenases), two

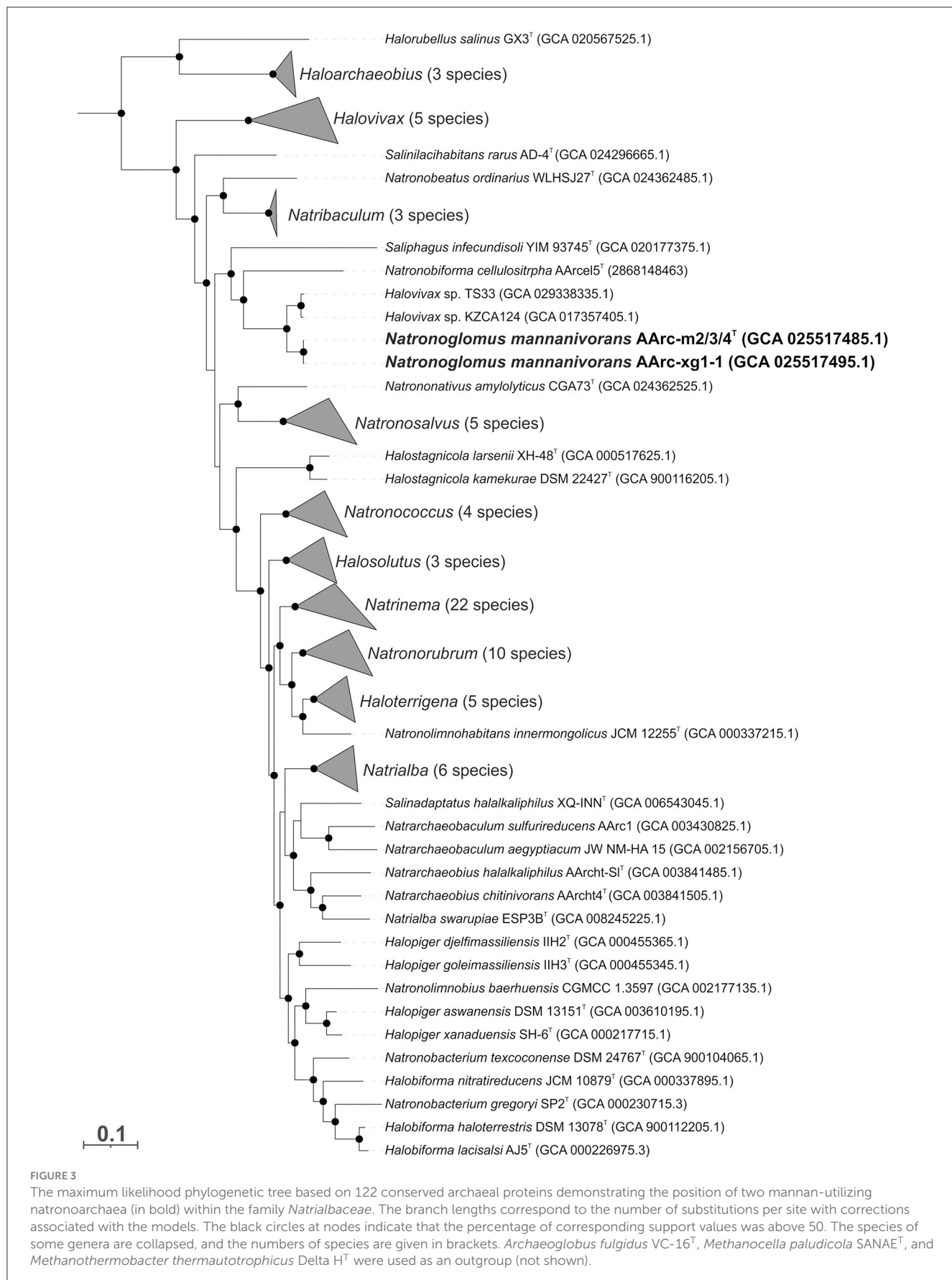


**TABLE 1** Polysaccharide hydrolases potentially involved in the beta-mannan, cellulose, and xylan hydrolysis encoded in the genome of mannan-utilizing strain AArc-m2/3/4.

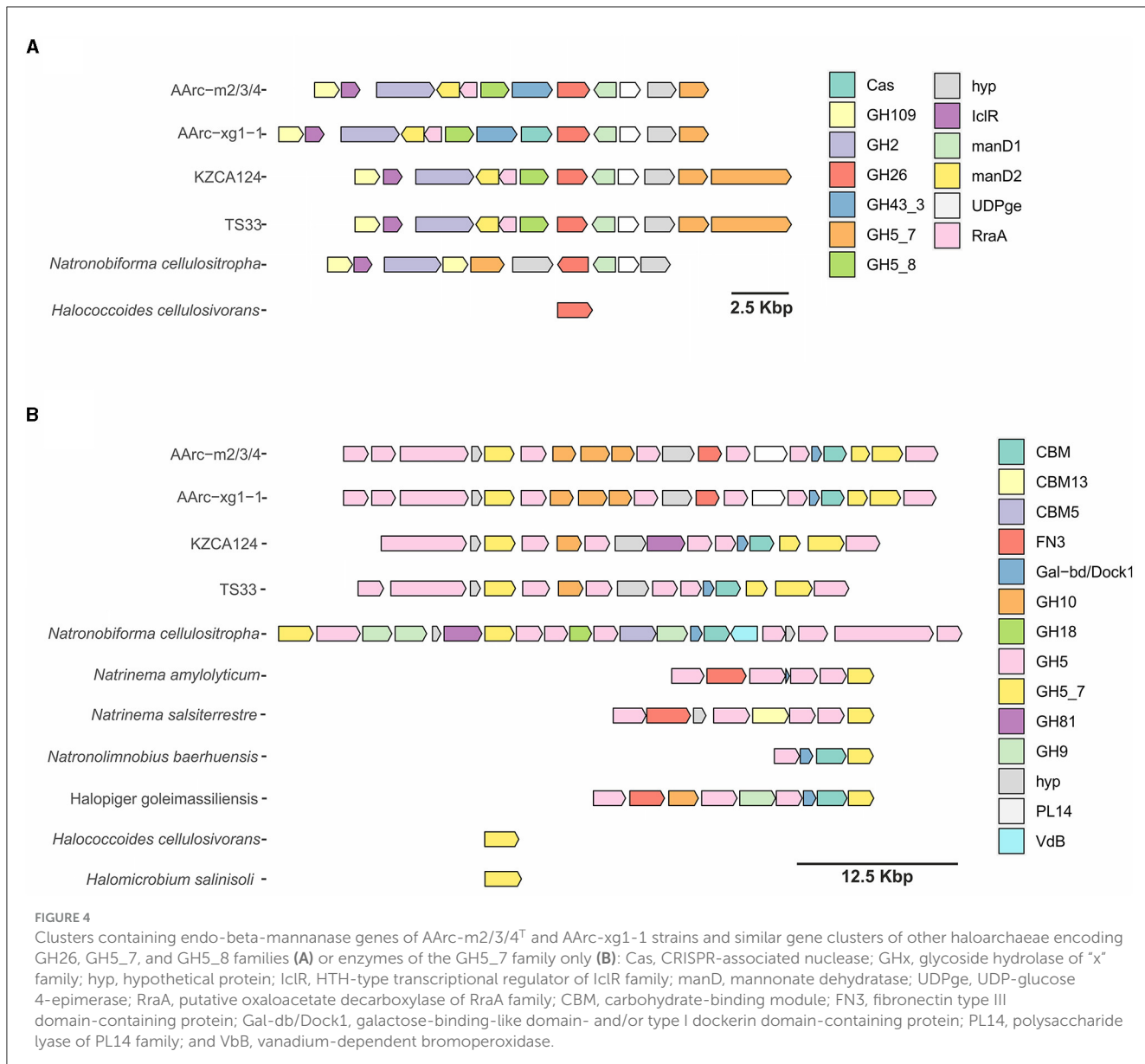
Locus tag MCU4972+	Protein family	Putative function	Protein size (aa)	Localization (signal peptide)
0716	GH5	Endo-beta-1,4-glucanase	523	(E) TAT/SPI
2295	GH11	Endo-beta-1,4-xylanase	428	(E) TAT/SPI
2297	GH10/2 × CBM85	Endo-beta-1,4-xylanase	1,035	(E) TAT/SPI-SPII
2716	GH5/PKD	Endo-beta-1,4-glucanase	637	(E) TAT/SPI
2717	GH5	Endo-beta-1,4-glucanase	610	(E) TAT/SPI
2718	GH5/CBM6	Endo-beta-1,4-glucanase	1,755	(E) TAT/SPI
2719	–	S-layer glycoprotein	258	(M) 2 TMH
2720	<b>GH5_7/CBM5</b>	<b>Endo-beta-1,4-mannanase</b>	759	(E) TAT/SPI
2721	GH5	Endo-beta-1,4-glucanase	646	(E) Sec/SPI
2722	GH10	Endo-beta-1,4-xylanase	589	(E) TAT/SPI
2723	GH10	Endo-beta-1,4-xylanase	741	(E) TAT/SPI
2724	GH10	Endo-beta-1,4-xylanase	577	(E) TAT/SPI
2725	GH5	Endo-beta-1,4-glucanase	600	(E) TAT/SPI
2726	–	Dockerin/PKD family	815	(E) TAT/SPI
2727	CBM6	Cellulose-binding	592	(E) TAT/SPI
2728	GH5	Endo-beta-1,4-glucanase	598	(E) TAT/SPI
2729	GH5/CBM6	Endo-beta-1,4-glucanase	835	(E) TAT/SPI
2730	GH5	Endo-beta-1,4-glucanase	490	(E) TAT/SPI
2732	CBM3	Chitin/cellulose-binding	578	(E) TAT/SPI
2733	<b>GH5_7</b>	<b>Endo-beta-1,4-mannanase</b>	469	(E) Sec/SPI
2734	<b>GH5_7</b>	<b>Endo-beta-1,4-mannanase</b>	779	(E) TAT/SPI
2735	GH5/CBM6	Endo-beta-1,4-glucanase	827	(E) TAT/SPI
3710	GH9	cellulase	821	(E) TAT/SPI
4111	GH5/CBM9	Endo-beta-1,4-glucanase	653	(E) TAT/SPI
5514	<b>GH5_7</b>	<b>Endo-beta-1,4-mannanase</b>	417	(E) TAT/SPI
5518	<b>GH26</b>	<b>Endo-beta-1,4-mannanase</b>	466	(E) TAT/SPI
5520	<b>GH5_8/CBM6</b>	<b>Endo-beta-1,4-mannanase</b>	407	(E) TAT/SPI
5524	GH2	Beta-mannosidase	844	(C)

(E), extracellular; (C), cytoplasmic; CBM, carbohydrate-binding domain. Mannan-specific enzymes are in bold.

mannanate dehydratases, putative UDP-glucose 4-epimerase, and a transcriptional regulator of the IclR family were encoded in this cluster. In the genome of AArc-xg1-1, there was an additional CRISPR-associated endonuclease. Very similar clusters were found in the genomes of undescribed strains KZCA124 and TS33, which were closely related to our mannan isolates, but they possessed an additional GH5\_7 gene, while genes of GH43 glycosidase were absent. Homologous cluster in *N. cellositropha* AArcl5 lacked genes of GH5\_8 enzyme and one mannanate dehydratase gene, while *Halococcoides cellosivorans* HArcl1 had only a single endo-beta-1,4-mannosidase from GH26.

The second cluster was much larger and encoded up to 21 proteins (Figure 4B). Identical clusters encoding 11 glycosides from the GH5 family (both endo-beta-1,4-mannanases and endoglucanases), three endo-beta-1,4-xylanases from the GH10

family, putative polysaccharide lyase (PL)14 with an unknown function, and several proteins containing putative CBM domains (galactose-binding-like domain, fibronectin type III, and type I dockerin) were observed in the genomes of AArc-m2/3/4 and AArc-xg1-1. Clusters in the genomes of KZCA124 and TS33 did not encode proteins of the PL14 family and fibronectin type III domain-containing proteins. Moreover, there were fewer genes of endo-glucanases from GH5 and GH10 enzymes. The largest endo-glucanase encoding cluster was found in the genome of *N. cellositropha* AArcl5 with 10 x GH5 and GH9 endo-beta-1,4-glucanases, GH81 endo-beta-1,3-1,4-glucanase but lack the GH10 xylanases. Other clusters of the second type consisted of four to nine genes (mostly genes of glycosidases from GH5 and GH5\_7). Both *H. cellosivorans* and *Halomicromobium salinisoli* had a single gene encoding endo-beta-1,4-mannanases from the GH5\_7 subfamily.



To predict the functions of the GH26 and GH5\_7/8 subfamilies more reliably, a phylogenetic analysis of these families was performed. This analysis demonstrated that the GH26 encoded in the genomes of the AArc-m2/3/4<sup>T</sup> and AArc-xg1-1 strains are indeed endo-beta-1,4-mannanases belonging to the clade containing biochemically characterized beta-mannanases from bacteria and fungi (Figure 5). In addition to the catalytic GH26 domain, these enzymes contain the dockerin type I domain participating in the binding of substrate. Enzymes of KZCA124 and TS33, as well as *N. cellulositropha* and *H. cellulosivorans*, also belong to this clade (II). It is remarkable that there were more than 100 proteins of the GH26 family from halophilic archaea (and other archaea) belonging to another clade (I), which have a very low level of homology with the confirmed beta-1,4-mannanases. It is likely that these proteins together with the characterized beta-1,3-xylanases should be separated into a different subfamily of the GH26 or even into a separate

family. Due to the complexity of the GH5 family, recently including 57 subfamilies (Supplementary Figure S3), analysis of these glycosidases was focused on clades containing endo-beta-mannosidases (GH5\_7 and GH5\_8 subfamilies). Both AArc-m2/3/4<sup>T</sup> and AArc-xg1-1 strains possess four enzymes from the GH5\_7 subfamily (Figure 6), of which two of them contained additional domains (carbohydrate-binding module family 5/12, fibronectin type III or PKD, and concanavalin A-like lectin domains), which may enhance the hydrolytic activity against insoluble polysaccharides. In addition to the abovementioned enzymes, KZCA124 and TS33 had another protein of GH5\_7 containing three fibronectin type III domains. Moreover, one enzyme of the GH5\_8 subfamily was encoded in each genome (Figure 7). These proteins consisted of a catalytic domain and the CBM5/12. Both GH5\_7 and GH5\_8 enzymes from the studied haloarchaea were clustered together with biochemically characterized endo-beta-1,4-mannanases from bacteria, fungi, and



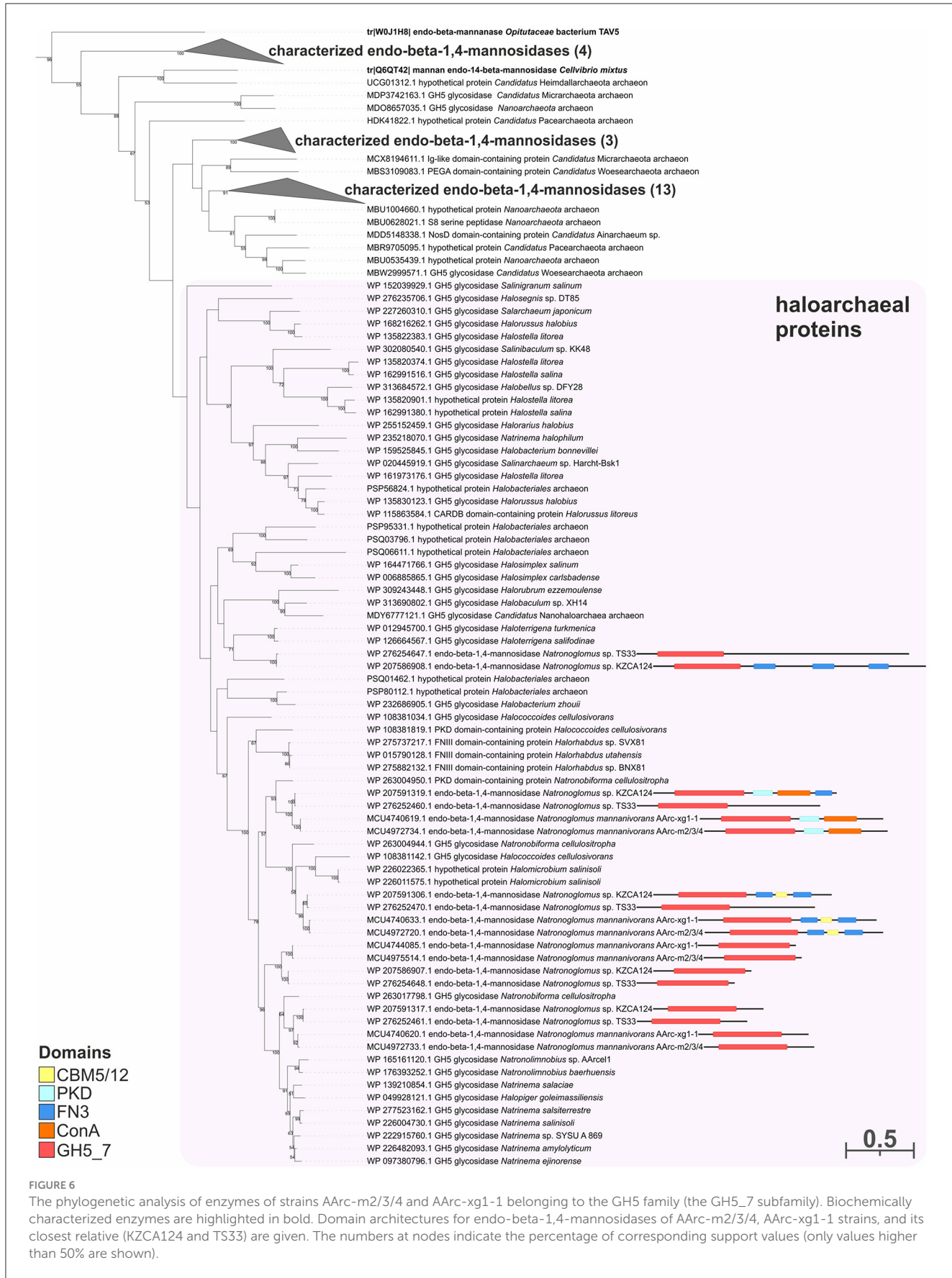
plants indicating that haloarchaeal proteins should also possess endo-mannanolytic activity.

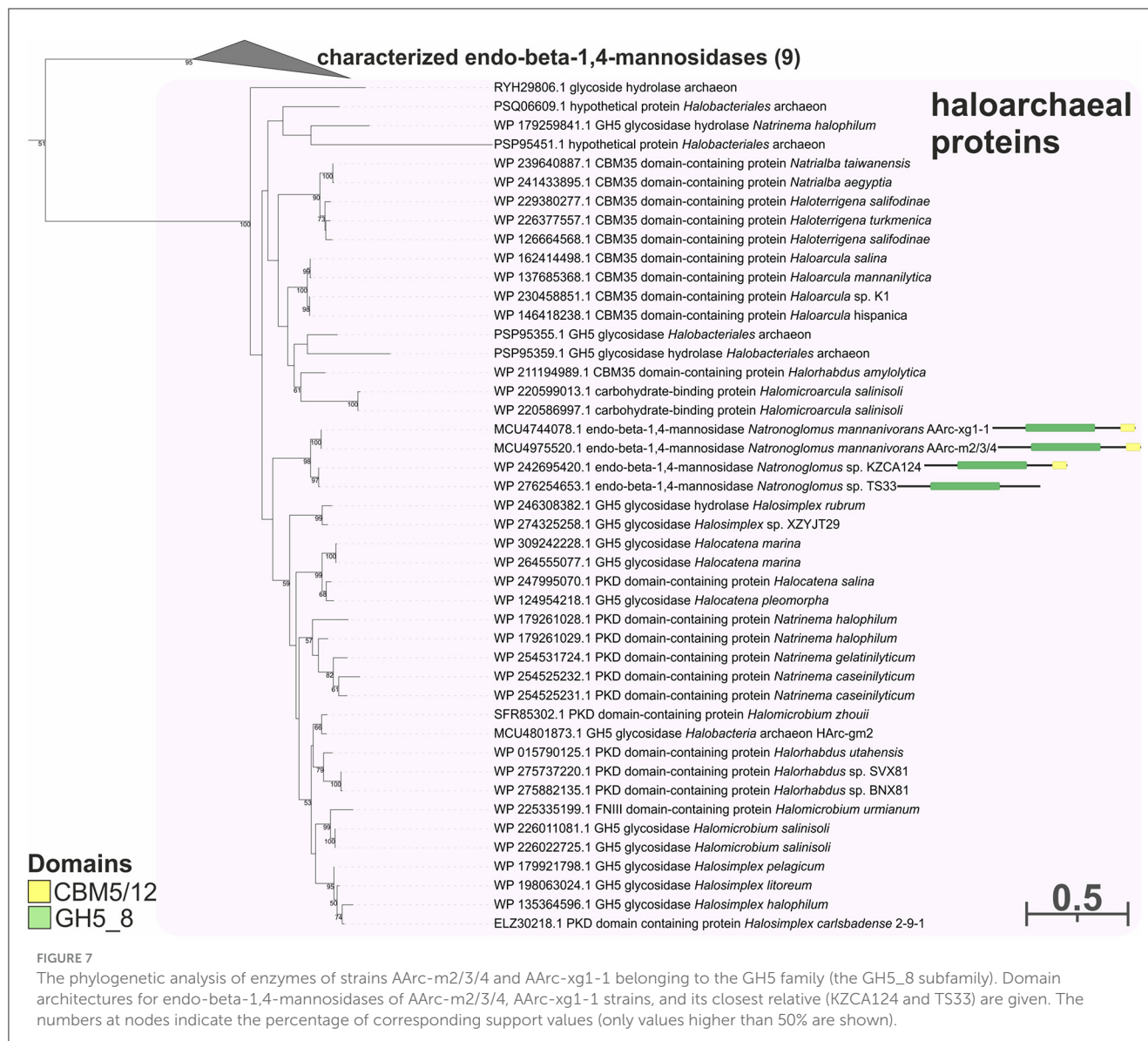
### Other repertoire of polysaccharide hydrolases encoded in the genomes

In addition to the mannanase-cellulase-xylanase GH families, both sequenced genomes also encoded a large repertoire of other polysaccharide-active enzymes including putative PL families listed in *Supplementary Tables S3* and *S4*. The major difference between these groups of hydrolases is cell localization: the former are generally all extracellular, while many proteins from the latter group are cytoplasmic. The putative substrate for such enzymes includes cellulose/xyloglucan (GH3, GH5, and GH9 families), xylan/arabinoxylan (GH3, GH10, GH11, GH51, GH67, and GH115 families) arabino-galactan (GH2, GH30, GH42, GH43, GH51, and GH154 families), starch (GH13 family), acidic polysaccharides, such as polygalacturonan (PL1, PL22, and GH28), rhamnogalacturonan (PL11, PL26, PL42, GH4, and GH105), and alginate, and their oligomers. However, growth and hydrolytic activity were only observed with arabinoxylan and xyloglucan.

### Central sugar metabolism

Taking into account that the GH2 family beta-mannosidases are intracellular and the strains are unable to grow on mannose, it is plausible to assume that mannan is hydrolyzed to mannooligosaccharides outside the cells, and then, the oligomers are imported into the cells. The phosphotransferase system (PTS) transporter genes were not found in the genomes of AArc-m2/3/4<sup>T</sup> and AArc-xg1-1 similar to cellulotrophic haloarchaea (Elcheninov et al., 2023). On the other hand, there were multiple genes of putative carbohydrate-specific ABC transporters (e.g., MCU4975802; 1351–1354; 1378–1381; 3422–3426; 4795.1–4797.1; 4083–4081; and 5056–5061) in AArc-m2/3/4<sup>T</sup>, some of which likely import mannooligosaccharides into the cells, and furthermore, they are hydrolyzed by the GH2 beta-mannosidases. It is likely that mannose is oxidized during the side activity of glucose dehydrogenase or putative oxidoreductase (MCU4975802) distantly homologous to mannose-specific aldohexose dehydrogenase from *Thermoplasma acidophilum* (Nishiya et al., 2004). Under the action of mannonate dehydratases ManD (the genes of two of them, 5517 and 5522, were co-located in the gene cluster with mannanases), mannose is converted





to 2-dehydro-3-deoxy-D-gluconate. Finally, it enters into the semi-phosphorylative Entner–Doudoroff (ED) pathway with the generation of glyceraldehyde-3-phosphate and pyruvate (Figure 8). Genes encoding enzymes of terminal steps in the ED pathway were also present: 2-dehydro-3-deoxy-D-gluconate kinase (3928 and 5533) and 2-dehydro-deoxy-6-phosphogluconate aldolase (2034).

### Other metabolically important traits

Other functionally important proteins from the genome of AArc-m2/3/4<sup>T</sup> are listed in Supplementary Table S5, including the ion-pH homeostasis, energy-related respiratory complexes, and some others. In particular, an incomplete denitrification pathway is encoded, including Cu-nitrite reductase NirK, archaeal type of NO-reductase qNor, and N<sub>2</sub>O reductase, but lacks nitrate reductase Nar. Despite this, the organisms did not grow anaerobically with either nitrite or N<sub>2</sub>O as acceptors (with cellobiose as substrate).

### Taxonomy conclusion

Comparative properties of the novel isolates in relation to the type species of the most related genera are shown in Table 2. The most similar in properties from the three related genera is obviously *N. cellulositropha*, but it was unable to grow with glucomannan and galactomannans, and its sugar utilization spectrum is much more restricted. The other two species of the related genera (*Natronosalvus* and *Saliphagus*) lack the beta-mannanase genes in their genomes and, thus, most likely would be able to grow with this polysaccharide type. In addition, *S. infecundisoli* is a neutrophilic haloarchaeon unable to grow at high pH. Furthermore, the mannan-utilizing natronoarchaea nearly lacked glycolipids, while in *Natronosalvus* and *Saliphagus*, several glycolipids constituted a large fraction of the membrane polar lipids, and the latter also has sulfolipid PGS not usually present in the soda lake natronoarchaea (Bale et al., 2021).

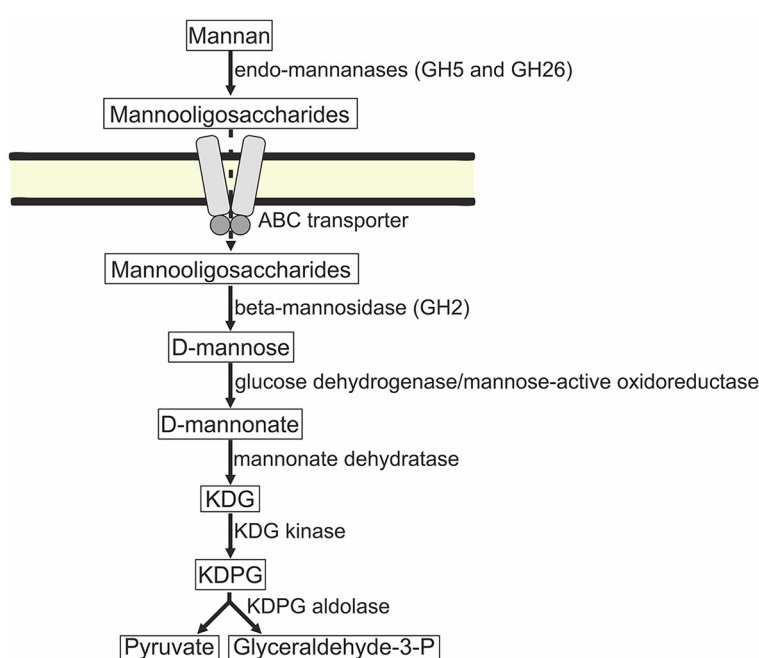


FIGURE 8

Predicted mannose catabolism pathway in strains AArc-m2/3/4 and AArc-xg1-1. ABC, ATP-binding cassette; KDG, 2-dehydro-3-deoxy-D-gluconate; KDPG, 2-dehydro-6-phosphogluconate.

In conclusion, taking into account the unique functional specialization and distant phylogeny, the beta-mannan-utilizing natronoarchaea from Siberian hypersaline soda lakes are proposed to form a new genus and species *Natronogloicus mannanivorans*.

## Description of *Natronogloicus mannanivorans* gen. nov., sp. nov.

### *Natronogloicus* gen. nov.

Na.tro.no.glo'mus. Gr. neut. n. *natron* arbitrarily derived from Arabic n. *natrun* or *natron*, soda; L. neut. n. *glomus*, a ball; N.L. neut. n. *Natronogloicus*, a coccoid natronoarchaeon.

Natronoarchaea from hypersaline lakes with mostly coccoid cells. Aerobic organoheterotrophs with the ability to utilize insoluble beta-mannans and cellulose as growth substrates. Extremely halophilic and moderately alkphilic. The dominant polar membrane lipids are phosphatidylglycerophosphate methyl ether (PGP-Me) and phosphatidylglycerol (PG) with C<sub>20</sub>-C<sub>20</sub> and C<sub>20</sub>-C<sub>25</sub> archaeol cores. The genus belongs to the *Natrialbaceae* family, class *Halobacteria*. A three-letter abbreviation is *Ngm*.

### *Natronogloicus mannanivorans* sp. nov.

man.na.ni.vo'rans. N.L. neut. n. *manna*num, mannan; L. pres. part. *vorans*, devouring; N.L. part. adj. *mannanivorans*, mannan devouring.

The cells are mostly non-motile cocci of 0.8–1.2 μm producing red pigments. The cells grown on mannan have a thick cell wall and extended pseudoperiplasm. The cells lyse in distilled water. The colony morphology varied depending on the substrate. On

insoluble polysaccharides, the colonies were mostly pale-pink, thin, spreading, and irregular, up to 4 mm; on soluble sugars, the colonies were pink, more regular, and convex, up to 3 mm. The core membrane diether lipids are dominated by C<sub>20</sub>-C<sub>20</sub> DGE (archaeol) and C<sub>20</sub>-C<sub>25</sub> DGE (extended archaeol). The polar lipid head groups include phosphatidylglycerolphosphate methyl ester (PGP-Me) and phosphatidylglycerol (PG). The dominant respiratory menaquinone is MK-8:8, with the MK-8:7 second in abundance. The species are obligatory aerobic saccharolytic heterotrophs that are able to grow with insoluble beta-1,4-mannan, glucosmannan, and cellulose. Sugars supporting the growth include galactose, rhamnose, raffinose, lactose, sucrose, cellobiose, maltose, trehalose, melezitose, and melibiose. Weak growth was observed on glycerol and pyruvate. Organic compounds tested (in the type strain) but not utilized included fructose, arabinose, ribose, xylose, sugar alcohols, acetate, ethanol, lactate, succinate, fumarate, malate, glycine, aspartate, glutamate, arginine, yeast extract, and peptone from casein. Ammonium and urea serve as the nitrogen source. Oxidase and catalase are positive. Mesophilic, with a maximum growth temperature of 48°C, is a low Mg-demanding, extreme halophile, with a range of Na<sup>+</sup> for growth from 2.5 to 4.5 M (optimum at 3.5 M), and a facultative alkophile, with a pH range from 6.8 to 9.6 for growth (optimum at 9–9.2). The G + C content of the DNA is 62% (two genomes), and the habitat is hypersaline salt lakes. The type strain (AArc-m2/3/4<sup>T</sup> = JCM 34861 = UQM 41565) was isolated from sediments of hypersaline soda lakes in the Kulunda Steppe (Altai, Russia). The species also includes other four closely related isolates, one of which is deposited in JCM (AArc-xg1-1 = JCM 34866). The draft genome assemblies' accession numbers of strains AArc-m2/3/4<sup>T</sup> and AArc-xg1-1 in the GenBank are GCA\_025517485 and GCA\_025517495.

TABLE 2 Comparative properties of the  $\beta$ -mannan utilizing isolates with the closest related genera from the family *Natrialbaceae* (Sorokin et al., 2018; Yin et al., 2018; Tan et al., 2023).

Property	<i>"Natronoglomus mannanivorans"</i>	<i>Natronobiforma cellulositropha</i>	<i>Natronosalvus amylolyticus</i>	<i>Saliphagus infecundisoli</i>
The number of isolates	5	4	1	2
Cell morphology	Non-motile cocci	Motile flat rods or non-motile cocci	Non-motile rods or angular coccoids	Non-motile cocci
Pigmentation	Red	Pink	Red	Pink-yellowish
Anaerobic growth	–	–	–	–
<b>Substrates for aerobic growth</b>				
Polysaccharides	Beta-mannans, cellulose, xylan, xyloglucan, and arabinoxylan	Cellulose, xylan, and beta-mannan	Starch	Starch
Sugars	Galactose, lactose, rhamnose, raffinose, sucrose, cellobiose, maltose, trehalose, melezitose, and melibiose	Cellobiose and maltose	Mannose, galactose, and sucrose	Glucose, mannose, raffinose, sucrose, maltose, and arachalose
Others	–	–	Pyruvate, alanine, and ornithine	Pyruvate, succinate, glutamate, aspartate, lysine, and ornithine
Beta-mannanase genes	+ (6)	+ (4)	–	–
Amylase	–	–	+	+
Esterase/lipase	– (tributyrin)	– (tributyrin)	– (Tween-80)	+(Tween-20)
Protease	– (casein)	– (casein)	+(casein)	+(casein)
Catalase/oxidase	+/-	+/-	nd	+/-
Indole from tryptophane	+	–	–	–
Salinity range (optimum) M Na <sup>+</sup>	2.0–4.5 (3.5)	2.5–4.8 (4.0)	0.9–4.8 (3.4)	2.0–6.0 (2.5–3.0)
pH range (optimum)	7.2–9.7 (9.0–9.2)	7.5–9.9 (8.5–9.0)	6.0–9.5 (8.0–8.5)	6.5–8.5 (7.0–7.5)
Temperature max (°C)	48 (at pH 8.5)	53 (at pH 8.5)	55*	50 (at optimum pH)
Core lipids (archaeols)	C <sub>20</sub> -C <sub>20</sub> , C <sub>20</sub> -C <sub>25</sub> DGE	C <sub>20</sub> -C <sub>20</sub> , C <sub>20</sub> -C <sub>25</sub> DGE	C <sub>20</sub> -C <sub>20</sub> , C <sub>20</sub> -C <sub>25</sub> DGE	nd
<b>Intact polar lipids</b>				
Phospholipids	PG, PGP-Me	PG, PGP-Me	PG, PGP-Me, PA	PG, PGP-Me, PGS
Glycolipids	MG (trace amount)	MG, DG	DGD-1, S-DGD-1 S-TGD-1	S-DGD-1
Respiratory lipoquinones	MK-8:8 (major) MK-8:7 (minor) MK-7:7 (trace amount)	nd	nd	nd
DNA G + C (% genomic)	62.0 (2 strains)	65.5 (1 strain)	63.7	64.0
Isolation source	Inland hypersaline salt and soda lakes	Inland hypersaline soda lakes	Hypersaline alkaline lake	Saline soil

nd, not reported.

\*The pH is not reported.

Lipids: PA, phosphatidic acid; PG, phosphatidylglycerol; PGP, phosphatidylglycerophosphate; PGP-Me, phosphatidyl-glycerophosphate methyl ester; PGS, phosphatidylglycerol sulfate; MG, phosphatidyl monoglycosyl diether; DG, phosphatidyl diglycosyl diether; DGD-1, mannosyl glycosyl diether; S-DGD-1, sulfated mannosyl glycosyl diether; S-TGD-1, sulfated galactosyl mannosyl glycosyl diether; and DGE, dialkyl glycerol ether.

## Data availability statement

The datasets presented in this study can be found in online repositories. The names of the repository/repositories and accession number(s) can be found in the article/[Supplementary material](#).

## Author contributions

DS: Conceptualization, Investigation, Writing—original draft. AE: Investigation, Writing—original draft. NB: Investigation, Writing—original draft. JS: Writing—original draft. IK: Writing—original draft.

## Funding

The author(s) declare financial support was received for the research, authorship, and/or publication of this article. All Russian authors were supported by the Russian Ministry of Higher Education and Science. DS was also partially supported by the Gravitation-SIAM Program of the Dutch Ministry of Education and Sciences (grant no. 24002002). NB and JS-D acknowledge support from the ERC Horizon 2020 Program (grant agreement no. 694569 – MICROLIPIDS).

## Conflict of interest

The authors declare that the research was conducted in the absence of any commercial or financial relationships that could be construed as a potential conflict of interest.

The author(s) declared that they were an editorial board member of Frontiers, at the time of submission.

This had no impact on the peer review process and the final decision.

## Publisher's note

All claims expressed in this article are solely those of the authors and do not necessarily represent those of their affiliated organizations, or those of the publisher, the editors and the reviewers. Any product that may be evaluated in this article, or claim that may be made by its manufacturer, is not guaranteed or endorsed by the publisher.

## Supplementary material

The Supplementary Material for this article can be found online at: <https://www.frontiersin.org/articles/10.3389/fmicb.2024.1364606/full#supplementary-material>

## References

- Aliyu, H., Lebre, P., Blom, J., Cowan, D., and De Maayer, P. (2016). Phylogenomic re-assessment of the thermophilic genus *Geobacillus*. *Syst. Appl. Microbiol.* 39, 527–533. doi: 10.1016/j.syapm.2016.09.004
- Bale, N. J., Ding, S., Hopmans, E. C., Villanueva, L., and Boschman, R. C. (2021). Lipidomics of environmental microbial communities. I: visualization of specific niches using untargeted analysis of high-resolution mass spectrometry data. *Front. Microbiol.* 12:659302. doi: 10.3389/fmicb.2021.659302
- Buchfink, B., Xie, C., and Huson, D. H. (2015). Fast and sensitive protein alignment using DIAMOND. *Nat. Methods* 12, 59–60. doi: 10.1038/nmeth.3176
- Capella-Gutiérrez, S., Silla-Martínez, J. M., and Gabaldón, T. (2009). trimAl: a tool for automated alignment trimming in large-scale phylogenetic analyses. *Bioinformatics* 25, 1972–1973. doi: 10.1093/bioinformatics/btp348
- Chaumeil, P. A., Mussig, A. J., Hugenholz, P., and Parks, D. H. (2019). GTDB-Tk: a toolkit to classify genomes with the genome taxonomy. *Bioinformatics* 36, 1925–1927. doi: 10.1093/bioinformatics/btz848
- de la Haba, R.R., Minegishi, H., Kamekura, M., Shimane, Y., Ventosa, A. (2021). Phylogenomics of *Haloarchaea*: the controversy of the genera *Natrinemata* and *Haloterrigena*. *Front. Microbiol.* 12:740909. doi: 10.3389/fmicb.2021.740909
- Elcheninov, A. G., Ugolkov, Y. A., Elizarov, I. M., Klyukina, A. A., Kublanov, I. V., Sorokin, D. Y., et al. (2023). Cellulose metabolism in halo(natrono)archaea: a comparative genomics study. *Front. Microbiol.* 14:111247. doi: 10.3389/fmicb.2023.111247
- Enomoto, S., Shimane, Y., Ihara, K., Kamekura, M., Itoh, T., Ohkuma, M., et al. (2020). *Haloarcula mannanilytica* sp. nov., a galactomannan-degrading haloarchaeon isolated from commercial salt. *Int. J. Syst. Evol. Microbiol.* 70, 6331–6337. doi: 10.1099/ijsem.0.004535
- Katoh, K., Rozewicki, J., and Yamada, K. D. (2017). MAFFT online service: multiple sequence alignment, interactive sequence choice and visualization. *Brief. Bioinform.* 20, 1160–1166. doi: 10.1093/bib/bbw108
- Letunic, I., and Bork, P. (2019). Interactive Tree Of Life (iTOL) v4: recent updates and new developments. *Nucleic Acids Res.* 47, W256–W259. doi: 10.1093/nar/gkz239
- Mistry, J., Finn, R. D., Eddy, S. R., Bateman, A., and Punta, M. (2013). Challenges in homology search: HMMER3 and convergent evolution of coiled-coil regions. *Nucleic Acids Res.* 41:e121. doi: 10.1093/nar/gkt263
- Nishiyama, Y., Tamura, N., and Tamura, T. (2004). Analysis of bacterial glucose dehydrogenase homologs from thermoacidophilic archaeon *Thermoplasma acidophilum*: finding and characterization of aldohexose dehydrogenase. *Biosci. Biotechnol. Biochem.* 68, 2451–2456. doi: 10.1271/bbb.68.2451
- Orata, F. D., Meier-Kolthoff, J. P., Sauvageau, D., and Stein, L. Y. (2018). Phylogenomic analysis of the gammaproteobacterial methanotrophs (order *Methylococcales*) calls for the reclassification of members at the genus and species levels. *Front. Microbiol.* 9:3162. doi: 10.3389/fmicb.2018.03162
- Paysan-Lafosse, T., Blum, M., Chuguransky, S., Grego, T., Pinto, B. L., Salazar, G. A., et al. (2023). InterPro in 2022. *Nucleic Acids Res.* 51, D418–D427. doi: 10.1093/nar/gkac993
- Qin, Q.-L., Xie, B.-B., Zhang, X.-Y., Chen, X.-L., Zhou, B.-C., Zhou, J., et al. (2014). A proposed genus boundary for the prokaryotes based on genomic insights. *J. Bacteriol.* 196, 2210–2215. doi: 10.1128/JB.01688-14
- Rinke, C., Chuvochina, M., Mussig, A. J., Chaumeil, P.-A., Davín, A. A., Waite, D. W., et al. (2021). A standardized archaeal taxonomy for the Genome Taxonomy Database. *Nat. Microbiol.* 6, 946–959. doi: 10.1038/s41564-021-00918-8
- Shimane, Y., Hatada, Y., Minegishi, H., Mizuki, T., Echigo, A., Miyazaki, M., et al. (2010). *Natronoarchaeum mannanilyticum* gen. nov., sp. nov., an aerobic, extremely halophilic archaeon isolated from commercial salt. *Int. J. Syst. Evol. Microbiol.* 60, 2529–2534. doi: 10.1099/ijss.0.016600-0
- Sorokin, D. Y., Elcheninov, A. G., Khijniak, T. V., Kolganova, T. V., and Kublanov, I. V. (2022a). Selective enrichment on a wide polysaccharide spectrum allowed isolation of novel metabolic and taxonomic groups of haloarchaea from hypersaline lakes. *Front. Microbiol.* 13:1059347. doi: 10.3389/fmicb.2022.1059347
- Sorokin, D. Y., Elcheninov, A. G., Toshchakov, S. V., Bale, N. J., Sinningshe Damsté, J. S., Khijniak, T. V., et al. (2019b). *Natrarchaeobius chitinivorans* gen. nov., sp. nov., *Natrarchaeobius halalkaliphilus* sp. nov., alkaliphilic, chitin-utilizing haloarchaea from hypersaline alkaline lakes. *Syst. Appl. Microbiol.* 42, 309–318. doi: 10.1016/j.syapm.2019.01.001
- Sorokin, D. Y., Elcheninov, A. S., Merkel, A. Y., Bale, N. J., Sinningshe Damsté, J. S., Kublanov, I. V., et al. (2023). *Halapricum hydrolyticum*, a beta-1,3-glucan utilizing haloarchaeon from hypersaline lakes. *Syst. Appl. Microbiol.* 46:126471. doi: 10.1016/j.syapm.2023.126471
- Sorokin, D. Y., Khijniak, T. V., Kostrikina, N. A., Elcheninov, A. G., Toshchakov, S. V., Bale, N. J., et al. (2018). *Natronobifirma cellulostropha* gen. nov., sp. nov., a novel haloalkaliphilic member of the family Natriabaceae (class Halobacteria) from hypersaline alkaline lakes. *Syst. Appl. Microbiol.* 41, 355–362. doi: 10.1016/j.syapm.2018.04.002
- Sorokin, D. Y., Khijniak, T. V., Kostrikina, N. A., Elcheninov, A. G., Toshchakov, S. V., Bale, N. J., et al. (2019a). *Halococcoides cellulosivorans* gen. nov., sp. nov., an extremely halophilic cellulose-utilizing haloarchaeon from hypersaline lakes. *Int. J. Syst. Evol. Microbiol.* 69, 1327–1335. doi: 10.1099/ijsem.0.03312
- Sorokin, D. Y., Toshchakov, S. V., Kolganova, T. V., and Kublanov, I. V. (2015). Natro(natrono)archaea isolated from hypersaline lakes utilize cellulose and chitin as growth substrates. *Front. Microbiol.* 6:942. doi: 10.3389/fmicb.2015.00942
- Sorokin, D. Y., Yakimov, M. M., Messina, E., Merkel, A. Y., Koenen, M., Bale, N. J., et al. (2022b). *Natranaeroarchaeum sulfidigenes* gen. nov., sp. nov., carbohydrate-utilizing sulfur-respiring haloarchaeon from hypersaline soda lakes, a member of a new family Natronoarchaeaceae fam. nov. in the order Halobacterales. *Syst. Appl. Microbiol.* 45:126356. doi: 10.1016/j.syapm.2022.126356

- Stamatakis, A. (2014). RAxML version 8: a tool for phylogenetic analysis and post-analysis of large phylogenies. *Bioinformatics* 30, 1312–1313. doi: 10.1093/bioinformatics/btu033
- Tan, S., Cheng, M., Li, X.-X., Hu, Y., Ma, X., Hou, J., et al. (2023). *Natronosalvus halobius* gen. nov., sp. nov., *Natronosalvus caseinilyticus* sp. nov., *Natronosalvus vescus* sp. nov., *Natronosalvus rutilus* sp. nov., *Natronosalvus amylolyticus* sp. nov., halophilic archaea isolated from salt lakes and soda lakes. *Int. J. Syst. Evol. Microbiol.* 73:006036. doi: 10.1099/ijsem.0.006036
- Wirth, J. S., and Whitman, W. B. (2018). Phylogenomic analyses of a clade within the *Roseobacter* group suggest taxonomic reassessments of species of the genera *Aestuarivivita*, *Citreicella*, *Loktanella*, *Nautella*, *Pelagibaca*, *Ruegeria*, *Thalassobius*, *Thiobacimonas* and *Tropicibacter*, and the proposal. *Int. J. Syst. Evol. Microbiol.* 68, 2393–2411. doi: 10.1099/ijsem.0.002833
- Yin, X.-Q., Liu, B.-B., Chu, X., Salam, N., Li, X., Wang, Z.-W., et al. (2018). *Saliphagus infecundisoli* gen. nov., sp. nov., an extremely halophilic archaeon isolated from a saline soil. *Int. J. Syst. Evol. Microbiol.* 67, 4154–4160. doi: 10.1099/ijsem.0.002270
- Zhang, H., Yohe, T., Huang, L., Entwistle, S., Wu, P., Yang, Z., et al. (2018). dbCAN2: a meta server for automated carbohydrate-active enzyme annotation. *Nucleic Acids Res.* 46, W95–W101. doi: 10.1093/nar/gky418

# ***Natronogloicus mannanivorans* gen. nov., sp. nov., beta-1,4-mannan utilizing natronoarchaea from hypersaline soda lakes**

Dimitry Y. Sorokin<sup>a,b\*</sup>, Alexander G. Elcheninov<sup>a</sup>, Nicole J. Bale<sup>c</sup>, Jaap Sininghe-Damste<sup>c</sup> and Ilya V. Kublanov<sup>a</sup>

<sup>a</sup>Winogradsky Institute of Microbiology, Research Centre of Biotechnology, Russian Academy of Sciences, Moscow, Russia

<sup>b</sup>Department of Biotechnology, Delft University of Technology, Delft, The Netherlands

<sup>c</sup>NIOZ Royal Netherlands Institute for Sea Research, Den Burg, Texel, The Netherlands

## **Supplementary files**

**Table S1.** Membrane polar lipids detected in strain AArc-m2/3/4.

**Table S2.** Whole genome comparison indexes between strains AArc-m2/3/4, AArc-xg1-1 and its closest representatives.

**Table S3.** Enzymes potentially involved in hydrolysis of various poly- and oligo-saccharides encoded in the genome of strain AArc-m2/3/4 (except for mannanases, cellulases and xylanases presented in the main text in **Table 1**).

**Table S4.** Complete repertoire of the CAZy enzymes encoded in the genomes of 2 mannan-utilizing natronoarchaea and closely related undescribed strains KZCA124 and TS33.

**Table S5.** A selection of functionally important proteins encoded in the genome of strain AArc-m2/3/4<sup>T</sup>.

**Fig. S1.** Colonial growth of beta-mannan utilizing natronoarchaea on insoluble beta-1,4-mannan (left column) and amorphous cellulose (right column) showing hydrolysis clearance zones around the colonies. **a-b**, strain AArc-m2/3/4; **c-d**, strain AArc-gm4; **e-f**, strain Aarc-glctm5; **g-h**, strain HArc-m1. The medium contained 4 M total Na<sup>+</sup> at pH 9.5, incubation time – 10-14 d at 37°C.

**Fig. S2.** Maximum likelihood phylogenetic tree based on 122 conserved archaeal proteins demonstrating position of two strains of mannan-utilizing natronoarchaea (in bold) within the family *Natrialbaceae*. The branch lengths correspond to the number of substitutions per site with corrections associated with the models. The numbers at nodes indicate that the percentage of corresponding support values. *Archaeoglobus fulgidus* VC-16<sup>T</sup>, *Methanocella paludicola* SANAE<sup>T</sup> and *Methanothermobacter thermautotrophicus* Delta H<sup>T</sup> were used as an outgroup (not shown).

**Fig. S3.** Phylogenetic analysis of enzymes of belonging to GH5 family. The numbers at nodes indicate that the percentage of corresponding support values (only values higher than 50% are shown). GH5\_7 and H5\_8 subfamilies are bounded with blue lines.

**Table S1.** Composition of intact polar lipids identified in strain AArc-m2/3/4<sup>T</sup>

Polar head group	Core	[M+H] <sup>+</sup>	Assigned elemental composition	% from total
PGP-Me	EXT-AR	971.7449	C <sub>52</sub> H <sub>109</sub> O <sub>11</sub> P <sub>2</sub>	10.1
	Uns(1)-EXT-AR	969.7286	C <sub>52</sub> H <sub>107</sub> O <sub>11</sub> P <sub>2</sub>	2.6
	Uns(2)-EXT-AR	967.7138	C <sub>52</sub> H <sub>105</sub> O <sub>11</sub> P <sub>2</sub>	1.3
	Uns(3)-EXT-AR	965.6976	C <sub>52</sub> H <sub>103</sub> O <sub>11</sub> P <sub>2</sub>	1.9
	Lyso-EXT-AR	691.3527	C <sub>32</sub> H <sub>69</sub> O <sub>11</sub> P <sub>2</sub>	0.6
	AR	901.6658	C <sub>47</sub> H <sub>99</sub> O <sub>11</sub> P <sub>2</sub>	30.7
	Lyso-AR	621.3527	C <sub>27</sub> H <sub>59</sub> O <sub>11</sub> P <sub>2</sub>	1.8
	<b>Total</b>			<b>49.0</b>
PG	EXT-AR	877.7623	C <sub>51</sub> H <sub>106</sub> O <sub>8</sub> P	14.3
	Uns(1)-EXT-AR	875.7461	C <sub>51</sub> H <sub>104</sub> O <sub>8</sub> P	2.5
	AR	807.6837	C <sub>46</sub> H <sub>96</sub> O <sub>8</sub> P	31.7
	Lyso-AR	527.3704	C <sub>26</sub> H <sub>56</sub> O <sub>8</sub> P	2.1
	<b>Total</b>			<b>50.6</b>
PG-Gly	Ext-AR	1039.815	C <sub>57</sub> H <sub>116</sub> O <sub>13</sub> P	<b>0.4</b>
	<b>Sum AR</b>			<b>27</b>
	<b>Sum EXT-AR</b>			<b>32</b>
	<b>Sum uns-EXT-AR</b>			<b>38</b>
	<b>Sum lyso-AR</b>			<b>3.3</b>

PGP-Me = phosphatidylglycerolphosphate methyl ester; PG = phosphatidylglycerol; PG-Gly= phosphatidylglycerohexose; AR = archaeol; (C<sub>20</sub>-C<sub>20</sub>); EXT-AR = extended archaeol (C<sub>20</sub>-C<sub>25</sub>); lyso = one alkyl chain is absent; uns = unsaturated.



**Table S3.**

Locus tag MCU4972+	Protein family	Putative function	Localization (signal peptide)
1417	GH3	beta-glycosidase	C
1587	GH105	alpha-rhamnogalacturonyl hydrolase	C
1683	GH15	Glucoamylase	C
1684	GH13_20	Maltogenic alpha-amylase	C
2278	GH5	Putative xyloglucan-specific glucanase	E (TAT/SPI)
2279	GH31_4	alpha-xylosidase	C
2298	GH67	alpha-glucuronidase	C
2305	GH3	beta-glycosidase	C
2307	GH4	alpha-glycosidase	C
2308	GH10	beta-1,4-xylanase	C
2327	GH42	beta-galactosidase	C
2328	PL42	rhamnose-alpha-1,4-glucuronate lyase	C
2490	GH43_3/CBM13	beta-galactofuranosidase	E (TAT/SPI)
2564	GH3	beta-glycosidase	C
3085	GH15	glucoamylase	C
3255	GH93	exo-alpha-arabinofuranosidase	C
3417	GH51_1	arabinan-exo-alpha-1,3- arabinofuranosidase	C
3418	GH2	alpha-arabinopyranosidase	C
3421	GH43_3	beta-galactofuranosidase	E (Sec-TAT/SPII)
3427	GH2	alpha- arabinopyranosidase	C
3431	GH127	beta-arabinopyranosidase	C
3461	GH28	alpha-galacturonase	C
3474	PL1_2	Pectate lyase	E (TAT/SPI)
3476	PL1_2		
3506	CBM13	Xylan-binding domain	E (TAT/SPI)
3507	GH2	beta-glycosidase	E (TAT/SPI)
3508	GH2		
3509	PL26	Rhamnogalacturonan exo-lyase	C
3513	GH28	alpha-galacturonase	C
3532	PL22	Oligogalacturonate lyase	C
3533	2 x PL22		
3537	GH78/CBM67	Rhamnogalacturonan alpha-rhamnosidase	C
3538	CBM13	Carbohydrate-binding domain	E (TAT/SPI)
3540	GH51_1	Arabinan-exo-alpha-1,3- arabinofuranosidase	C
3541	GH106	Rhamnogalacturonan alpha-rhamnohydrolase	C
3543	2 x PL22	Oligogalacturonate lyase	C
3545	GH43	alpha-arabinanase	C
3549	GH95	alpha-galacto/fucosidase	C
3550	GH43_18	alpha-arabinofuranosidase	C
3552	PL11_1	Rhamnogalacturonan lyase	C
3555	GH78/CBM67	Rhamnogalacturonan alpha-rhamnosidase	C
3556; 3558	GH2	beta-galacturonidases	C
3562	GH42	beta-galactosidase	C
3563	2 x CBM13	Carbohydrate-binding domain	E (TAT/SPI)
3677	GH43_12/CBM91	beta-xylosidase	C
3844	GH32	Levansucrase/inulinase	C

3845	GH154	beta-1,6-glucuronidases	C
3874	CBM88	Xyloglucan/galactomannan-specific CBM	E (TAT/SPI)
4048; 4050; 4057	GH2	beta-galactosidases	C
4079	GH88	beta-glucuronyl hydrolase	C
4103	GH95	alpha-fucosidase/galactosidase	
4104	GH29	alpha-fucosidase/galactosidase	C
4109	GH2	beta-galactosidase	C
4265	GH3	beta-glucosidase	C
4344	GH43_12/CBM91	beta-xylosidase	
4345	GH159	alpha-arabinofuranosidase	C
4390	GH4	alpha-gluco/galactosidase	C
5260	GH51_1	arabinan-exo-alpha-1,3- arabinofuranosidase	E (TAT/SPII)
5300	GH28	alpha-galacturonase	C
5301	2 x PL22	Oligogalacturonate lyase	C
5302	CBM9	Cellulose-binding domain	C
5303	GH115	alpha-1,6-glucuronidase	C
5305	GH4	alpha-galacturonidase	C
5308	GH78/CBM67	Rhamnogalacturonan alpha-rhamnosidase	C
5309	CBM13	Carbohydrate-binding domain	E (TAT/SPI)
5450	GH88	Xyloglucan/galactomannan-specific CBM	C
5456	GH29	alpha-fucosidase/galactosidase	C
5457	GH137	beta-arabinofuranosidase	C
5461	2 x GH2	beta-galactosidases	
5462	GH2	beta-galactosidases	C
5469	GH29	alpha-fucosidase/galactosidase	C
5470	GH2	beta-galactosidases	C
5481	GH78/CBM67	Rhamnogalacturonan alpha-rhamnosidase	C
5482	GH106	Rhamnogalacturonan alpha-rhamnohydrolase	C
5485; 5491	GH78/CBM67	Rhamnogalacturonan alpha-rhamnosidase	C
5519	GH43_3/CBM13	endo-alpha-arabininase	E (TAT/SPI)
5556	GH3	beta-glycosidase	C
5789	GH95	alpha-fucosidase/galactosidase	C
5961;5962; 5964	GH29	alpha-fucosidase/galactosidase	C

(E), extracellular; (C), cytoplasmic







# TS33

Gene ID	HMMER	dbCAN_sub	DIAMOND	Function
WP_276252459.1	GH5(64-356)+CBM6(516-654)	GH5_e197+CBM6_e47	CBM6+GH5	endo-1,4-beta-glucanase
WP_276252460.1	<b>GH5_7(92-385)</b>	<b>GH5_e4</b>	<b>GH5_7</b>	<b>endo-1,4-beta-mannosidase</b>
WP_276252461.1	<b>GH5_7(92-381)</b>	<b>GH5_e4</b>	<b>GH5_7</b>	<b>endo-1,4-beta-mannosidase</b>
WP_276252462.1-		-	CBM5	cellulose-binding CBM
WP_276252464.1	GH5(66-370)	GH5_e197	GH5	endo-1,4-beta-glucanase
WP_276252465.1	GH5(91-392)	GH5_e92	GH5	endo-1,4-beta-glucanase
WP_276252467.1	GH5(109-415)	GH5_e92	GH5	endo-1,4-beta-glucanase
WP_276252468.1	GH10(113-449)	GH10_e16	GH10	endo-1,4-beta-xylanase
WP_276252469.1	GH5(49-497)	GH5_e197	GH5	endo-1,4-beta-glucanase
WP_276252470.1	<b>GH5_7(97-385)</b>	<b>GH5_e4</b>	<b>CBM5+GH5_7</b>	<b>endo-1,4-beta-mannosidase</b>
WP_276252472.1	GH5(68-409)	GH5_e197	GH5	endoglucanase
WP_276252473.1	GH5(61-465)	GH5_e92	GH5	endoglucanase
WP_276252597.1	GH3(90-314)	GH3_e181	GH3	beta-glucosidase/beta-xylosidase
WP_276252658.1	GH10(3-213)	GH10_e16	-	endo-1,4-beta-xylanase
WP_276252661.1	CBM57(88-224)	CBM57_e32	-	broad-specificity CBM
WP_276252663.1	GH10(50-367)	GH10_e16	GH10	endo-1,4-beta-xylanase
WP_276252664.1	GH43_3(46-348)+CBM13(374-513)	GH43_e112+CBM13_e196	CBM13+GH43_3	endo-alpha-1,5-L-arabinanase
WP_276252754.1	GH2(22-582)	GH2_e67	GH0	beta-galactosidase
WP_276253105.1	GH95(6-734)	GH95_e1	GH95	alpha-L-fucosidase
WP_276253111.1	GH29(3-369)	GH29_e0	GH29	alpha-L-fucosidase
WP_276253115.1	GH95(11-738)	GH95_e1	GH95	alpha-L-fucosidase
WP_276253116.1	PL1_2(90-260)	PL1_e72	PL1	pectate lyase
WP_276253173.1	PL12(345-479)	PL12_e12	PLO	heparin-sulfate lyase
WP_276253290.1	CBM6(208-343)	CBM6_e4	-	xylan-binding CBM
WP_276253291.1	PL14(156-358)	PL14_e16	-	alginate lyase
WP_276253293.1	PL14(25-229)	PL14_e16	-	alginate lyase
WP_276253309.1	CE15(19-396)	CE15_e20	CE15	4-O-methyl-glucuronoyl methylesterase
WP_276253409.1	GH4(3-181)	GH4_e21	GH4	alpha-galactosidase
WP_276253872.1	GH3(55-263)	GH3_e103	GH3	beta-glucosidase
WP_276253901.1	GH13(301-614)	GH13_e49	GH13	alpha-amylase
WP_276253902.1	GH15(292-649)	GH15_e46	GH15	alpha-amylase
WP_276253913.1	GH29(3-373)	GH29_e0	GH29	alpha-L-fucosidase
WP_276254039.1	CE19(42-387)	CE19_e4	-	pectin methylesterase
WP_276254127.1	GH105(40-342)	GH105_e35	GH105	unsaturated rhamnogalacturonyl hydrolase
WP_276254560.1	CE4(224-341)	CE4_e274	-	chitin deacetylase
WP_276254647.1	<b>GH5_7(91-372)</b>	<b>GH5_e4</b>	<b>GH5_7</b>	<b>endo-1,4-beta-mannosidase</b>
WP_276254648.1	<b>GH5_7(88-380)</b>	<b>GH5_e239</b>	<b>GH5_7</b>	<b>endo-1,4-beta-mannosidase</b>
WP_276254652.1	<b>GH26(50-339)</b>	<b>GH26_e17</b>	<b>CBM88+GH26</b>	<b>endo-1,4-beta-mannosidase</b>
WP_276254653.1	<b>GH5_8(96-291)</b>	<b>GH5_e158+CBM5_e73</b>	<b>GH5</b>	<b>endo-1,4-beta-mannosidase</b>
WP_276254656.1	<b>GH2(3-706)</b>	<b>GH2_e94</b>	<b>GH2</b>	<b>beta-mannosidase</b>
WP_276254678.1	GH27(96-358)	GH27_e14	GH27	alpha-galactosidase
WP_276254680.1	GH3(86-315)	GH3_e181	GH3	beta-glucosidase/beta-xylosidase
WP_276254736.1	GH9(112-611)	GH9_e1	GH9	endo-1,4-beta-glucanase
WP_276254969.1	PL42(28-333)	PL42_e0	PL42	rhamnose-alpha-1,4-gucuronate lyase
WP_276254993.1	GH11(62-235)+CBM13(262-398)	GH11_e15+CBM13_e122	CBM13+GH11	endo-1,4-beta-xylanase
WP_276254994.1	CBM85(106-240)+CBM85(329-461)+GH10(520-834)	CBM85_e8+CBM85_e8+GH10_e16	CBM85+GH10	endo-1,4-beta-xylanase
WP_276254995.1	GH67(8-688)	GH67_e1	GH67	alpha-1,2-glucuronosidase
WP_276255002.1	GH3(93-319)	GH3_e88	GH3	beta-xylosidase/beta-glucosidase
WP_276255004.1	GH4(30-207)	GH4_e30	GH4	alpha-galacturonidase
WP_276255006.1	GH10(8-321)	GH10_e102	GH10	endo-1,4-beta-xylanase
WP_276255016.1	GH31(221-716)	GH31_e10	GH31	alpha-xylosidase
WP_276255017.1	GH5(66-369)	GH5_e197	GH5	endo-1,4-beta-glucanase
WP_276255134.1	GH159(36-252)	GH159_e6	GH159	alpha-arabinofuranosidase/beta-galactofuranosidase
WP_276255183.1	GH43_14(3-298)+CBM91(334-512)	GH43_e73+CBM91_e27	GH43_12	alpha-L-arabinofuranosidase
WP_276255396.1	GH4(3-181)	GH4_e21	GH4	alpha-galactosidase
WP_276255415.1	CE6(121-225)+CBM88(306-395)	CE6_e3	CBM5+CE6	carbohydrate acetyl esterase/feruloyl esterase
WP_276255588.1	CE12(192-378)	CE12_e31	CE12	rhamnogalacturonan acetylesterase
WP_276255624.1	GH3(43-254)	GH3_e103	GH3	beta-glucosidase
WP_276255695.1	PL11(1-575)	PL11_e0	CBM13+PL11_1	rhamnogalacturonan lyase
WP_276255813.1	GH88(43-378)	GH88_e1	GH88	unsaturated glucuronyl hydrolase
WP_276255844.1	CE19(36-331)	CE19_e1	-	pectin methylesterase

WP_276255845.1 GH28(69-445)	GH28_e139	GH28	polygalacturonase
WP_276255863.1 PL22_2(189-381)	PL22_e6	PL22	oligogalacturonide lyase
WP_276255864.1 PL22(45-149)+PL22_2(180-374)	PL22_e5+PL22_e6	PL22	oligogalacturonide lyase
WP_276255866.1 CBM13(165-303)	CBM13_e294	-	mannose-binding CBM
WP_276255867.1 CBM67(119-313)+GH78(333-863)	CBM67_e11+GH78_e42	GH78	alpha-L-rhamnosidase
WP_276255870.1 GH51(226-720)	GH51_e48	GH51	alpha-L-arabinofuranosidase
WP_276255871.1 GH106(13-774)	GH106_e6	GH106	alpha-L-rhamnosidase
WP_276255873.1 PL1_2(483-665)	PL1_e72	PL1	pectate lyase
WP_276255876.1 PL22(48-154)+PL22(196-399)	PL22_e5+PL22_e6	PL22	oligogalacturonide lyase
WP_276255880.1 GH95(7-797)	GH95_e1	GH95	alpha-L-fucosidase
WP_276255881.1 GH43_18(43-277)	GH43_e83	GH43_18	alpha-L-arabinofuranosidase
WP_276255882.1 PL22(45-144)	PL22_e5+PL22_e6	PL22	oligogalacturonide lyase
WP_276255884.1 CBM13(552-683)	CBM13_e294	CBM13	mannose-binding CBM
WP_276255888.1 CBM67(332-481)+GH78(545-1068)	CBM67_e28+GH78_e58	GH78	alpha-L-rhamnosidase
WP_276255889.1 GH2(6-579)	GH2_e144	GH2	beta-glucuronidase/beta-galactosidase
WP_276255890.1 PL26(279-786)	PL26_e0	-	rhamnogalacturonan lyase
WP_276255893.1 GH2(2-740)	GH2_e145	GH2	beta-galactosidase
WP_276255895.1 GH43_3(47-334)	GH43_e110	CBM13+GH43_3	endo-alpha-1,5-L-arabinanase
WP_276255896.1 GH42(6-385)	GH42_e1	GH42	beta-galactosidase
WP_276255897.1 CBM13(398-509)+CBM13(487-557)	CBM13_e196	CBM13	mannose-binding CBM
WP_276255899.1 CE12(7-214)	CE12_e12	CE12	rhamnogalacturonan acetylesterase
WP_276255906.1 GH2(8-558)	GH2_e59	GH2	beta-glucuronidase
WP_276255944.1 PL1_2(77-261)+PL1_2(563-741)+PL1_2(1055-1239)	PL1_e72+PL1_e72+PL1_e72	PL1	pectate lyase
WP_276255959.1 GH28(33-389)	GH28_e10	GH28	polygalacturonase
WP_276255960.1 PL1_2(432-615)	PL1_e72	PL1	pectate lyase
WP_276255991.1 GH127(15-550)	GH127_e0	GH127	beta-L-arabinofuranosidase
WP_276255992.1 GH2(4-691)	GH2_e86	GH2	beta-galactosidase/beta-glucuronidase
WP_276255998.1 GH51(3-504)	GH51_e19	GH51	alpha-L-arabinofuranosidase
WP_276256021.1 CE14(17-126)	CE14_e40	-	diacetylchitobiose deacetylase
WP_276256033.1-	-	CEO	putative CE
WP_276256048.1 PL33(411-552)	PL33_e14	PL33_2	putative PL33
WP_276256079.1 GH32(24-322)	GH32_e85	GH32	sucrose-6-phosphate hydrolase
WP_276256080.1 GH154(11-359)	GH154_e14	GH154	beta-1,6-D-glucuronidase
WP_276256114.1 CBM13(424-566)	CBM13_e196	CBM13	mannose-binding CBM
WP_276256221.1 CE14(8-117)	CE14_e40	-	diacetylchitobiose deacetylase
WP_276256223.1 GH13_31(33-394)	GH13_e122	GH13_31	oligo-1,6-glucosidase
WP_276256226.1 GH97(3-592)	GH97_e8	GH97	alpha-galactosidase
WP_276256271.1 CBM13(173-313)	CBM13_e122	-	mannose-binding CBM
WP_276256272.1 GH2(61-833)	GH2_e101	GH2	beta-galactosidase
WP_276256273.1 GH2(7-482)	GH2_e41	GH2	beta-glucuronidase/beta-galactosidase
WP_276256275.1 GH2(6-565)	GH2_e144	GH2	beta-glucuronidase
WP_276256284.1 GH154(11-351)	GH154_e14	GH154	beta-1,6-D-glucuronidase
WP_276256370.1 CE15(84-403)+CE15(442-777)	CE15_e17+CE15_e17	CEO	4-O-methyl-glucuronoyl methyl esterase
WP_276256392.1 CE14(6-115)	CE14_e40	-	chitin deacetylase
WP_276256395.1 GH20(147-472)	GH20_e51	GH20	beta-hexosaminidase
WP_276256399.1 GH3(77-303)	GH3_e204	GH3	beta-hexosaminidase
WP_276256401.1 GH20(152-477)	GH20_e51	GH20	beta-hexosaminidase
WP_276256402.1-	-	PLO	putative PL
WP_276256420.1 GH20(129-442)	GH20_e75	GH20	beta-hexosaminidase
WP_276256459.1 CE14(9-118)	CE14_e40	-	chitin deacetylase
WP_276256465.1 PL11(1-591)	PL11_e0	PL11_1	rhamnogalacturonan lyase
WP_276256467.1 PL1_2(386-554)	PL1_e72	PL1	putative PL1
WP_276256582.1 GH97(3-580)	GH97_e29	GH97	alpha-galactosidase
WP_276256591.1 GH97(28-680)	GH97_e24	GH97	alpha-glucosidase
WP_276256607.1 GH42(8-398)+GH164(304-656)	GH42_e24+GH164_e0	GH42	beta-galactosidase
WP_276256616.1 GH99(3-289)	GH99_e4	-	endo-alpha-1,2-mannosidase
WP_276256619.1 GH38(97-374)	GH38_e13	GH38	alpha-mannosidase
WP_276256621.1 GH38(7-289)	GH38_e33	GH38	alpha-mannosidase
WP_276256622.1-	-	GH38	alpha-mannosidase
WP_276256625.1 GH141(15-547)	GH141_e24	GH141	alpha-L-fucosidase/xylanase
WP_276256649.1 GH33(17-265)	GH33_e136	GHO	putative GH33
WP_276256653.1 <b>GH2(17-759)</b>	<b>GH2_e94</b>	<b>GH2</b>	<b>beta-mannosidase</b>
WP_276256656.1 GH38(274-527)	GH38_e38	GH38	alpha-mannosidase

WP_276256657.1-	-	GH38	alpha-mannosidase
WP_276256658.1 GH38(7-289)	GH38_e33	GH38	alpha-mannosidase
WP_276256659.1 GH29(22-369)	GH29_e83+CBM32_e149	CBM32+GH29	alpha-L-fucosidase
WP_276256660.1 GH29(3-353)	GH29_e0	GH29	alpha-L-fucosidase
WP_276256663.1 GH20(130-383)	GH20_e75	GH20	beta-hexosaminidase
WP_276256664.1 GH29(4-351)	GH29_e54	GH29	alpha-L-fucosidase
WP_276256675.1 GH18(20-316)	GH18_e66	GH18	endo-chitinase
WP_276256688.1 GH33(303-595)	GH33_e4	GH33	putative GH33
WP_276256692.1 CBM9(16-212)	-	-	xylan-binding CBM
WP_276256702.1 GH171(23-388)	GH171_e0	GH171	beta-N-acetyl muramidase
WP_276256708.1 GH171(22-388)	GH171_e0	GH171	beta-N-acetyl muramidase
WP_276256822.1 GH3(80-303)	GH3_e1	GH3	beta-glucosidase/beta-xylosidase
WP_276256823.1 GH144(45-442)	GH144_e3	GH144	endo-beta-1,2-glucanase
WP_276256825.1 GH172(87-329)	GH172_e0	GH172	difructose dianhydride I synthase/hydrolase
WP_276256828.1 CBM67(6-174)+GH78(237-734)	CBM67_e16+GH78_e57	CBM67+GH78	alpha-L-rhamnosidase
WP_276256835.1-	CBM13_e294	CBM0+PL11_1	rhamnogalacturonan lyase
WP_276256844.1 CBM67(363-516)+GH78(576-1084)	CBM67_e28+GH78_e58	GH78	alpha-L-rhamnosidase
WP_276256847.1 GH4(20-200)	GH4_e30	GH4	alpha-galacturonidase
WP_276256849.1 GH115(21-970)	GH115_e6	GH115	xytan alpha-1,2-glucuronidase
WP_276256850.1 CBM9(17-222)	-	-	xytan-binding CBM
WP_276256851.1 PL22(30-153)+PL22_2(198-376)	PL22_e5+PL22_e6	PL22	oligogalacturonate lyase
WP_276256852.1 GH28(28-390)	GH28_e40	GH28	polygalacturonase
WP_276256884.1 GH51(5-484)	GH51_e44	GH51	alpha-L-arabinofuranosidase
WP_276257005.1 CE4(221-340)	CE4_e274	-	chitin deacetylase CE4
WP_276257014.1 GH2(36-940)	GH2_e61	GH2	beta-galactosidase
WP_276257091.1 GH5(47-315)+CBM9(469-641)	GH5_e92+CBM9_e5	CBM9+GH5	endoglucanase
WP_276257093.1 GH42(6-392)	GH42_e1	GH42	beta-galactosidase
WP_276257099.1 GH2(6-580)	GH2_e127	GH2	beta-galactosidase/beta-glucuronidase
WP_276257120.1 GH38(274-528)	GH38_e18	GH38	alpha-mannosidase
WP_276257139.1 CBM13(231-366)	CBM13_e31	CBM13	mannose-binding CBM

**Table S5.**

Protein subunits	Protein name/function	Locus tag (MCU497+)
<b>Ion/pH homeostasis</b>		
TrkAH locus	Trk system: K <sup>+</sup> /H <sup>+</sup> symporter	4800-4809
TrkA_C-terminal	Potassium import : single subunits	2522-2523; 3340; 5908
TrkA_N-terminal		2524; 2622; 3163
KdpAB/ TrkAH	High-affinity K <sup>+</sup> -uptake ATPase/ Potassium symporter	5901-5902/ 5903-5904
CPA2	K <sup>+</sup> /H <sup>+</sup> antiporter	1449; 1718
KefB	K <sup>+</sup> /H <sup>+</sup> antiporter (efflux)	1717
Kch PchB Two-pore channel	Potassium channels	1397 3702 1167
NatAB1B2	Na <sup>+</sup> -efflux ABC transporter	1569-1561
<b>Ca/Mg uptake</b>		
CaCA	Ca <sup>+</sup> /Na <sup>+</sup> antiporter	2699; 3161; 5166
MtgE	Magnesium transporter	1398-1399; 3648-3649
<b>Na<sup>+</sup>/H<sup>+</sup> antiporters</b>		
NhaP	Single subunit Na(K) <sup>+</sup> /H <sup>+</sup> antiporter	1720; 4800
MrpB1B2CD1D2D3EFG	multisubunit Na <sup>+</sup> /H <sup>+</sup> antiporter	4115-4123
<b>Oxidative stress response components</b>		
KatG	Catalase/peroxidase HPI	1889
KatE	Catalase	5270
AhpD	Alkylperoxidase	1633
Bcp	PeroxiredoxinQ	1964
Sod	[Mn] superoxide dismutase	1592; 5621
<b>Respiratory cytochrome complexes</b>		
heme-copper cytochrome <i>c</i> oxidase <i>aa</i> <sub>3</sub>		
CoxD/B/AC	Catalytic subunit IV/II/I-III	3230/3253/3302
cytochrome <i>c</i> /quinol oxidase <i>ba</i> <sub>3</sub>		
CbaA1B/CbdA/TlpA/CSO	Subunit I-II/cytochrome c biogenesis	5683-5687
CbaEDA2C	Catalytic subunits III-V	5809-5812
CtaB/Cox10	Heme <i>o</i> synthase	3407; 5690
CtaA/Cox15	Heme <i>a</i> synthase	1395
<b>NADH-MK oxido-reductase</b>		
PetABDE	Haloarchaeal complex III	4564-4568
<b>Aerobic type of CO-dehydrogenase</b>		
CoxSML/I	Mo-Cu CO dehydrogenase	1179-1182
<b>Denitrification</b>		
HpcE/ NirK	Plastocyanin/Cu-nitrite reductase	5688-5689
NorZ (qNorB)	Archaeal NO-reductase	5222
NosL1Y1F1DL2/Z	N <sub>2</sub> O-reductase operon1	3623-3628
NosF2Y2L3	N <sub>2</sub> O-reductase operon2	5815-5817
<b>Periplasmic halocyanin/plastocyanin Cu-proteins (replacements for cytochrome <i>c</i>)</b>		
Hcy	Halocyanin family	1867; 2083; 3906
HcpE	Plastocyanin/azurin family	1806; 2124-2126; 3339; 4564; 4612
GlbN	Cyanoglobin (truncated hemoglobin)	2335
UrtABCD	Urea ABC transporter	3492-3495
UreABC	Urease catalytic subunits	3496-3498
UreDEFG	Urease accessory proteins	3498-34502
PhaCEP	Archaeal PHA synthase type III	5584-5586

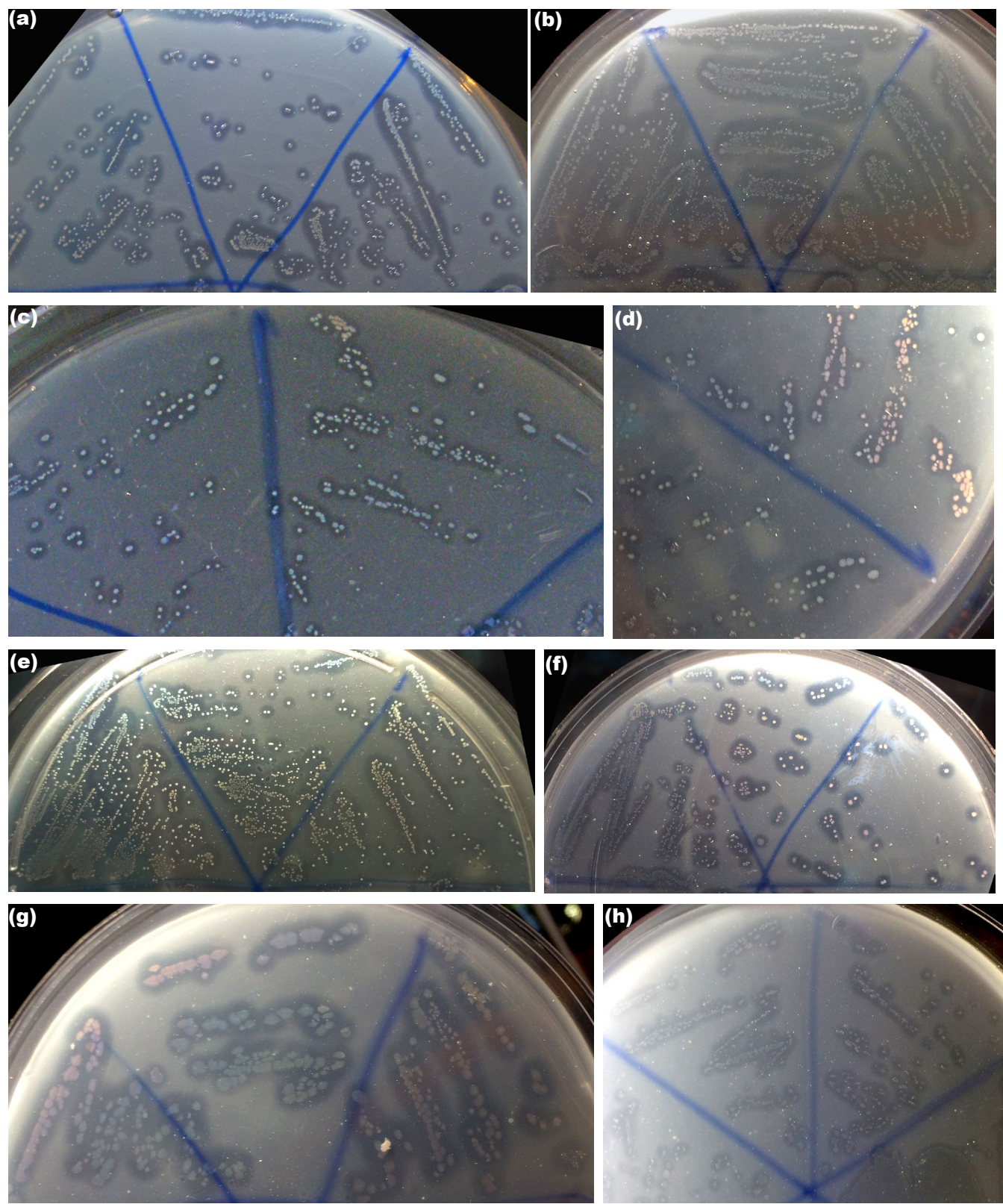


**Fig.S1**

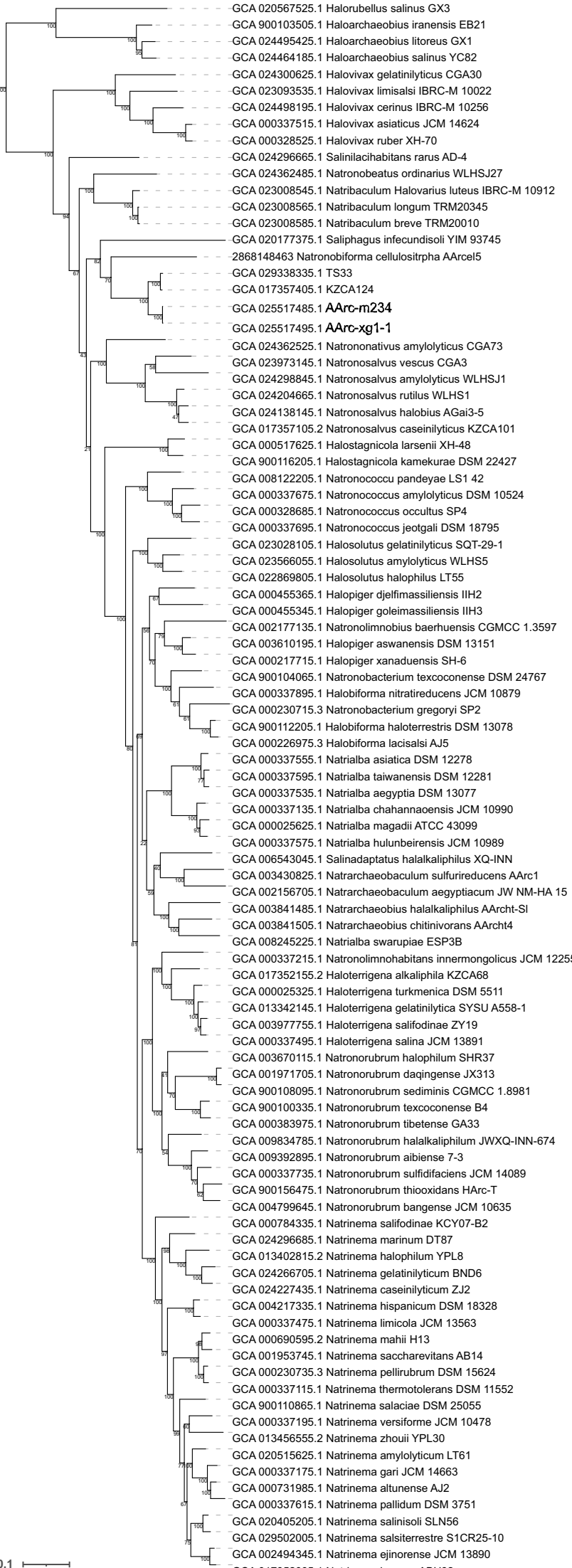
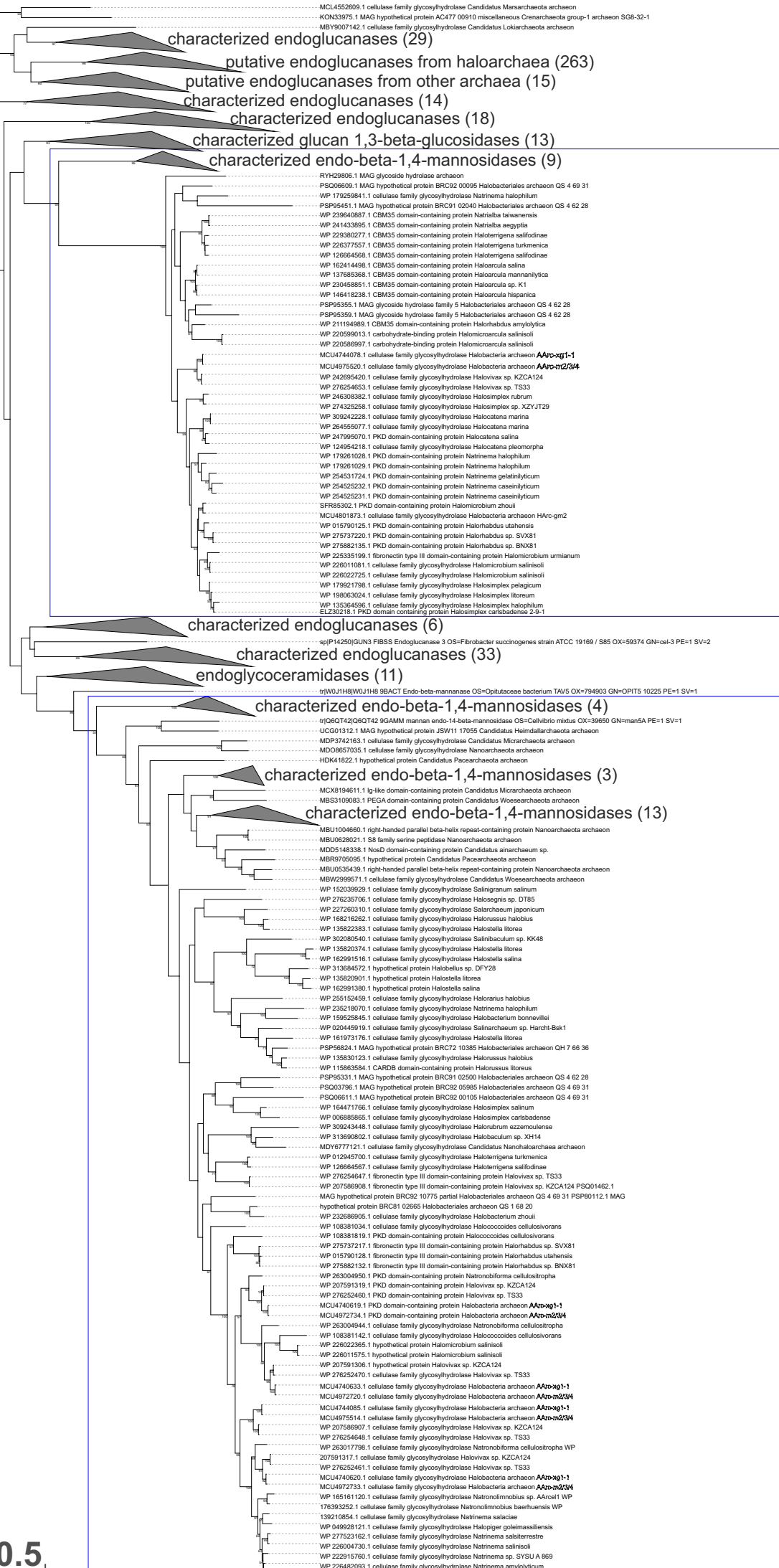


Figure S2



## GH5\_7

Figure S3